Alma Mater Studiorum - Università di Bologna

SCUOLA DI SCIENZE

Dipartimento di Chimica Industriale "Toso Montanari"

Corso di Laurea Magistrale in

Chimica Industriale

Classe LM-71 - Scienze e Tecnologie della Chimica Industriale

New W-doped nickel aluminate catalysts in the glycerol hydrodeoxygenation (HDO)

Tesi di laurea sperimentale

CANDIDATO

Irene Sinisgalli

RELATORE

Prof.ssa Patricia Benito Martin

CORRELATORE

Prof. Jose Luis Ayastuy

Anno Accademico 2020-2021

Abstract

Biorefineries are emerging as an important pillar for achieving both sustainable energy and chemicals. Bio-derived feedstocks are extremely various, but one of the most relevant building block chemicals coming from them is glycerol. Glycerol is an interesting molecule to be valorised because of its high functionalization degree and the huge surplus obtained from biodiesel production. Among all the possible valorisation routes, the catalytic Aqueous-Phase Hydrodeoxygenation (APHDO) allows to combine two processes (APR and HDO) and to overcome the issues related to normal glycerol HDO, conducted with external and high-pressure H_2, by producing H_2 *in-situ* via APR on part of the reactant itself.

This thesis work is focused on the development of a new catalytic system for the APHDO based on Ni, known to be active on APR, and doped with W, which increase the acidity of the system and makes it active towards HDO. Effects of dopant loading, synthesis method and space velocity were evaluated. To evaluate the effect of doping, four catalysts with different W loadings were synthetised via sol-gel method, characterised trough a wide range of analytical techniques (XRD, XRF, H_2-TPR, NH_3-TPD, N_2 physisorption and H_2 chemisorption), and their catalytic activity was tested in a continuous tubular reactor, at 235 °C and 45 bar. Afterwards, the catalyst that showed the best performance among them was prepared through impregnation method and was characterised and tested as before. Finally, the Weight Hourly Space Velcoity (WHSV) effect was studied by conducting the process under the same conditions and with a doubled glycerol feeding flow. W-doping resulted to be effective in HDO activation, giving low values of carbon conversion to gas, and the catalytic performance resulted to be influenced by the preparation method. Low WHSV values resulted to be better for a good interaction between the substrate of the reaction and the catalyst.

Keywords

Glycerol, Aqueous-Phase Hydrodeoxygenation, *in-situ* hydrogen, nickel aluminate spinel, high value-added liquid products.

Acronyms and abbreviations

APHDO: Aqueous-Phase Hydrodeoxygenation

APR: Aqueous-Phase Reforming

ATR: Autothermal Reforming

BET: Brunauer-Emmet-Teller

CHT: Catalytic Transfer Hydrogenation

D_{Ni}: Dispersion of metallic nickel

DDO: Degree of deoxygenation

EG: Ethylene glycol

FWMH: Full Width Half Maxima

GC-FID: Gas Chromatography – Flame Ionization Detector

GHGs: Green House Gases

HA: Hydoxyacetone

HDO: Hydrodeoxygenation

H_2-TPR: H_2-Temperature Programmed Reduction

IC: Inorganic Carbon

ICDD: International Centre for Diffraction Data

IUPAC: International Union of Pure and Applied Chemistry

NDIR: Non Dispersive Infra Red

NH_3-TPD: NH_3-Temperature Programmed Desorption

PDO: Propanediol

PG: Propylene glycol

POR: Partial Oxidation Reforming

S_{BET}: BET Surface

SC_i: Carbon Selectivity

SCWR: Super Critical Water Reforming

SESR: Sorbent Enhanced Steam Reforming

SR: Steam Reforming

TC: Total carbon

TCD: Thermal Conductivity Detector

TGA: Thermogravimetric Analysis

VOCs: Volatile Organic Compounds

WHSV: Weight Hourly Space Velocity

WGS: Water-Gas Shift

XRD: X-Ray Diffraction

XRF: X-Ray Fluorescence

3-HPA: 3-Hydroxypropionaldehyde

d_P: Diameter of the particle

X_{gas}: Carbon conversion to gas

X_{gly}: Conversion of total glycerol

Greek letters

β: Line broadening at half the maximum intensity, rad

η: Efficiency

λ: Wavelength of the x-ray, nm

θ: Diffraction angle, °

τ: Dimension of the crystallite, Å

TABLE OF CONTENTS

Live as if you were to die tomorrow.
Learn as if you were to live forever.

(Mahatma Ghandi)

1. INTRODUCTION

1.1 CONTEXT OF THE RESEARCH

The current and strongly based on fossil fuels energy model is not economically nor environmentally sustainable anymore since industrialization and population are increasing, together with the need for energy. In addition, not only energy carriers come from petroleum refineries, but also the dependence of chemicals production on fossil resources is even stronger. Nowadays, price of fossil resources is increasing while fossil reserves are decreasing. Besides, their use contributes to increase the atmospheric pollution, leading to huge emissions of GHGs (Green House Gases), SO_x, NO_x, CO, VOCs (Volatile Organic Compounds) and particulate matter[1]. For all these reasons, in order to simultaneously reduce the dependence on oil and mitigate the climate change, alternative production chains are necessary, which must imply the use of renewable and less impacting resources. It is increasingly and globally being recognized that for this purpose, for a future sustainable economy, biomass has the potential to replace a large fraction of fossil resources as feedstocks for industrial productions, addressing both the energy and non-energy (i.e. chemicals and materials) sectors. Indeed, from a technical point of view, almost all the fuels and chemicals normally made out from petroleum can be produced starting from these bio-based feedstocks in the so-called biorefineries, as shown in ***Figure 1***.

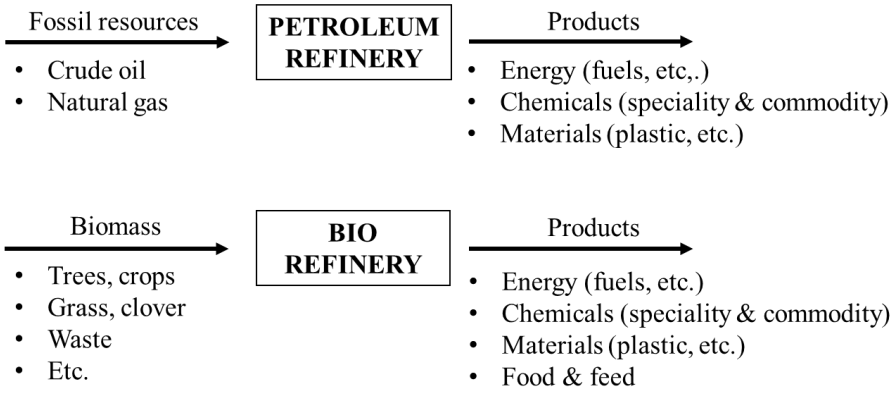

Figure 1*. Comparison between petrorefinery and biorefinery.*

Because of the high oxygen content, biomass, to be valorised, needs to be depolymerized and deoxygenated[2]: the high ratio O/C of the molecules makes them not perfectly suitable for fuel and chemical applications because of low energy density, potentially high acidity, and possible

by-products formation. In general, the production of high value-added chemicals (platform chemicals) requires a lower deoxygenation degree than the production of biofuels, since the presence of oxygen very often provides valuable physical and chemical properties to the product, but it is still necessary. Among various valorisation pathways, catalytic conversion is a promising approach to aid biorefinery economics[3]. In the light of this, to use biomass as raw material and to develop new, more efficient, and environmentally friendly processes, the research on design of highly active and selective catalysts has been boosted. Indeed, biomass conversion with high atom efficiency is a key aspect to compete with petroleum refineries in the production of high value-added bio-based chemicals and fuels.

Considering all the possible advantages of bio-refinery, the European Union (EU) declared the bio-based products sector as a priority area with high potential for future growth, reindustrialisation, and addressing societal challenges. In this sense, biorefining integrated in the Circular Economy concept is the optimal strategy for large-scale sustainable use of biomass in the so-called Bioeconomy.

1.2 GLYCEROL

Glycerol is included in the top twelve building block chemicals derived from biomass, which can be valorised through bio-refinery[4]. It is a representative platform molecule typically obtained as by-product of processes on triglycerides, like transesterification of oils and fats, soap manufacture or fatty acid production. The reaction of transesterification of a triglyceride is reported as example in ***Figure 2***.

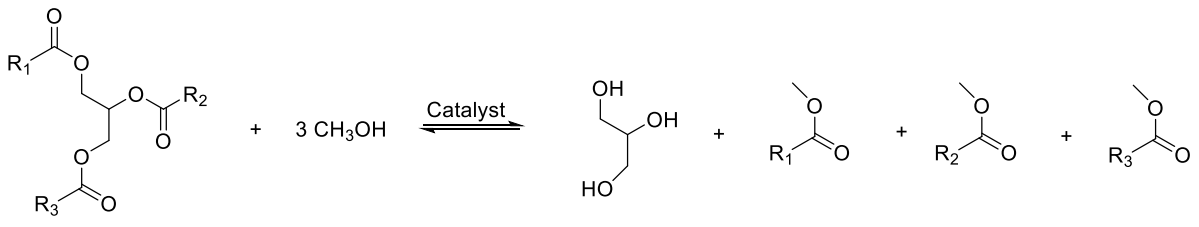

Figure 2*. Transesterification of a triglyceride with methanol.*

A big fraction of glycerol is also formed during biodiesel production as major by-product: approximately 10 wt. % of the total biodiesel produced is glycerol, which means that approximately 110 kg per ton of biodiesel produced can be considered waste stream. In the last

years, with the notable increase in the use of biodiesel, an abundant stock of surplus glycerol is being produced. Thus, for the economic viability of biodiesel industries and the improvement of biorefineries efficiency, it is necessary to recycle this chemical into higher value-added products.

1.2.1 Properties of glycerol

Glycerol (1,2,3-propanetriol, ***Figure 3***) is a colourless, odourless, and viscous liquid with a sweet taste. It is fully soluble in water and alcohols, slightly soluble in many common solvents (such as ether and dioxane) and is totally insoluble in hydrocarbons. Its physical and chemical properties (***Table 1***) make it a very versatile organic compound.

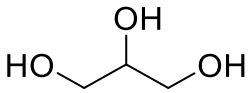

Figure 3*. Structure of glycerol.*

Table 1*. Physicochemical properties of glycerol at 20 °C.*

Chemical formula	$C_3H_3(OH)_3$
Molecular mass	92.09382 g/mol
Density	1.261 g/cm^3
Viscosity	1.5 Pa.s
Melting point	18.2 °C
Boiling point	290 °C
Food energy	4.32 kcal/g
Flash point	160 °C
Surface tension	64.00 mN/m
Temperature coefficient	-0.0598 mN/(mK)

1.2.2 Commercial applications

Thanks to its physicochemical properties, glycerol presents more than a thousand uses and applications, either directly as an additive or as a raw material. Glycerol finds its main applications as solvent, sweetener and preservative in food and beverages. It is then used as softener and plasticizer to impart flexibility, pliability, and toughness. Another important use is

as humectant, a substance for retaining moisture and giving, at the same time, softness; glycerol is, indeed, able to draw water from the surroundings and to produce heat by absorption, warming itself up. Thanks to its hygroscopic property it is also used in adhesive and glues to keep them from drying too quickly. Finally, thanks to the lubrication power, many uses can be mentioned in cosmetics as carriers and emollients, and in medical and pharmaceutical preparations. In general, however, only low concentrations of glycerol are employed in these applications, which are unable to absorb the large surplus of biodiesel-generated glycerol on the market. Research and industries have been investigating new uses for glycerol and, in relatively few years, there have been lots of achievements. Many different valorisation routes are possible thanks to the high functionalization of the molecule, that presents three vicinal hydroxyl groups, and this is also why it is rapidly establishing itself as a major platform to produce chemicals and fuels[5]. Some of the routes are better explained in section 1.3.

1.3 GLYCEROL VALORIZATION ROUTES

1.3.1 Selective oxidation

Selective oxidation is particularly interesting because of the commercial importance of oxygenated glycerol derivatives (***Figure 4***). Previously, only the biological transformation of glycerol was known, and hydroxyacetone was the only product to be generated. The development of new catalytic systems permitted to obtain various new derivatives and many examples are here reported[6]:

- New gold catalysts provided the basis for a high selective process for glyceric acid production.
- Conventional platinum and palladium catalysts, in new bi- and poli- metallic systems, were discovered to be very useful in the intensive oxidation of glycerol to mesoxalic and tartronic acids.
- Electrochemical oxidation in fuel cells was found to be able to complete the cycle of conversion of renewable seed oil to energy.

Glyceraldehyde represents a standard for relative enantiomeric configurations, and it also has a role as intermediate in carbohydrate metabolism. Hydroxyacetone is as a synthon for organic synthesis and is used in artificial tanning. Glyceric and hydroxypyruvic acids are promising

monomers for new polymeric materials and chelating agents. Mesoxalic and tartronic acids are interesting pharmaceutical precursors.

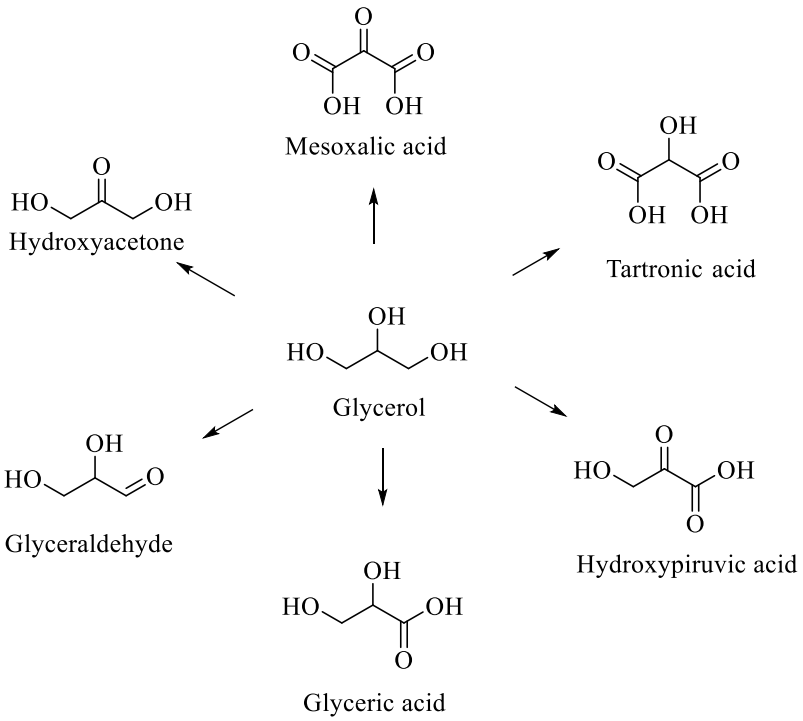

***Figure 4**. Oxidized glycerol derivatives.*

The progress in oxidation technology marks the increasing importance of the use of green processes, possibly carried out under mild conditions and using molecular oxygen in aqueous solutions. Another example in this direction is the development of some heterogeneous systems, in which a solid catalyst is stirred with liquid reactants in the presence of oxygen or, even better, air, simplifying the separation of the catalysts from the products and, furthermore, speeding up the purification of the final products.

1.3.2 Dehydration

Acrolein and 3-hydroxypropionaledehyde (3-HPA) are the main chemicals that can be produced by glycerol dehydration. In general, dehydration to acrolein (***Figure 5***) is carried out under acidic conditions, since when protonated glycerol has a lower energy barrier than the normal one (20 kJ/mol vs. 60 kJ/mol). Furthermore, dehydration reaction is favoured by high temperatures and/or partial vacuum, which push the reaction in the direction of water loss. The

reaction may be so conducted in liquid or gaseous phase, at temperatures around 250 – 340 °C, and catalysed by acids.

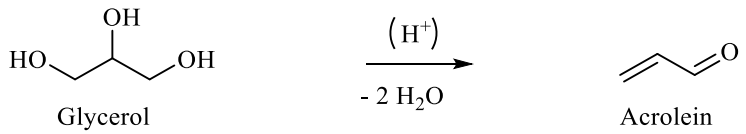

Figure 5. *Acid-induced dehydration of glycerol to acrolein.*

Production of 3-HPA (***Figure 6***) is instead a biotechnological process, which can be carried out using an aqueous solution of glycerol either at room temperature or 37 °C under atmospheric pressure. The transformation is a one-step enzymatic reaction and has a yield of about 85 % mol.

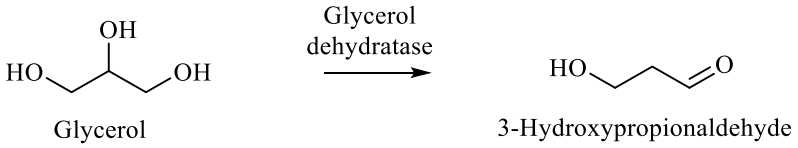

Figure 6. *Biotechnological dehydration of glycerol to 3-hydrpxypropionaldehyde.*

Importance to acrolein is given by the fact that it is the starting point to produce several important end-products, like plastic monomers (such as acrylic acid for the production of acrylic resins or other super-absorbent polymers), mono-alcohols, and energy gases (such as propane, used for green Liquefied Petroleum Gas, LPG). 3-Hydroxypropionaledehyde is very important as intermediate, since it is quite easy to convert into a lot of commodity chemicals, including acrolein, 3-hydroxipropionic acid, acrylic acid, malonic acid, and acrylamide, used for polymeric production. 3-HPA is also used as food preservative and as therapeutic auxiliary agent in the pharmaceutical industry, since it shows antimicrobial activity towards plenty of pathogens and food spoilage organisms.

1.3.3 Hydrogenolysis

The hydrogenolysis reaction of glycerol aims to selectively cleave C–O and C-C bonds, depending on the final product to be obtained. Similar to other conventional hydro-treating processes, glycerol hydrogenolysis usually requires elevated temperatures (> 220 °C) and H_2

pressures (> 4 MPa)[7]. In the presence of metallic catalysts, milder conditions can be used, and glycerol can be selectively hydrogenated to propylene glycol (PG), ethylene glycol (EG) and 1,3-propanediol (PDO) (***Figure 7***). From a commercial point of view, production of propylene glycol is one of the most important achievements of the new glycerol chemistry, since it is a relevant commodity chemical normally derived from crude petroleum oil.

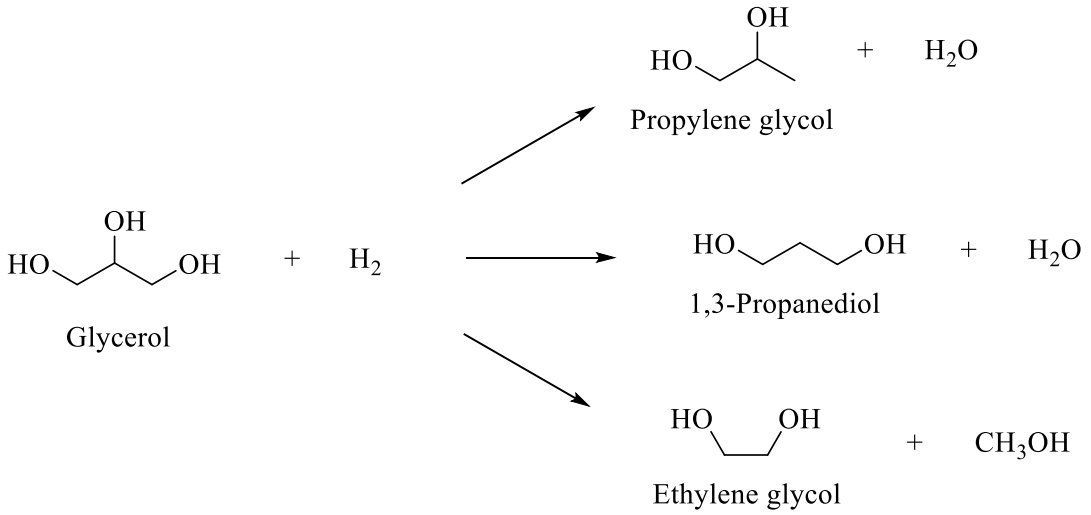

Figure 7*. Conversion of glycerol to propylene glycol, ethylene glycol and 1,3-propanediol.*

A screening study of catalysts has shown that, the key factor to achieve high selectivity towards propylene glycol from glycerol hydrogenolysis is the synergy of highly dispersed noble metals and oxophilic metals. Indeed, noble metals can activate H_2 to provide the hydrogen source for the hydrogenolysis reaction, while oxophilic metals are able to absorb glycerol thanks to the interaction with oxygen. To summarise, noble metals provide the active H_2 that then, by mean of hydrogen spillover, reaches the surface of the oxophilic metals where the glycerol is adsorbed, and the C-O bond is cleaved[8].

1.3.4 Aqueous-Phase Reforming (APR)

The Aqueous-Phase Reforming (APR) reaction transforms oxygenated compounds, as glycerol, in a gas phase composed mainly by H_2 and CO. It represents an attractive alternative for hydrogen production due to the many advantages over traditional methods (i.e., steam reforming), like the lower energy consumption. Since the reactants do not need to be vaporized, low temperatures (around 250 °C) can be used, and this can also prevent parallel reactions like decomposition of the starting materials. Undesired products, such as alcohols or organic acids,

can, indeed, be formed by breaking off the C-O bonds or by hydrogenation of CO and CO_2, with consequent formation of CH_4 and other alkanes, as shown in equations *(1.1)* and *(1.2)*, both reactions of methanation, and in equation *(1.3)*, Fischer-Tropsch synthesis.

$$CO + 3\,H_2 \rightleftharpoons CH_4 + H_2O \qquad (1.1)$$

$$CO_2 + 4\,H_2 \rightleftharpoons CH_4 + 2\,H_2O \qquad (1.2)$$

$$(2n + 1)\,H_2 + n\,CO \rightleftharpoons C_nH_{2n+2} + n\,H_2O \qquad (1.3)$$

In order to avoid these side reactions, it is important to use catalysts which are more selective for hydrogen production, thus, more active in the cleavage of C-C, C-H and O-H bonds, and which are also able to promote the removal of adsorbed CO by Water-Gas Shift (WGS) reaction, improving this way the formation of the product of interest.

The global reaction of APR is generally described by the equation *(1.4):*

$$C_3H_8O_3 + 3\,H_2O \longrightarrow 3\,CO_2 + 7\,H_2 \qquad (1.4)$$

which can be seen as the combination of two sub-reactions: the decomposition of glycerol *(1.5)* and the Water Gas Shift *(1.6).*

$$C_3H_8O_3 \longrightarrow 4\,H_2 + 3\,CO \qquad (1.5)$$

$$CO + H_2O \rightleftharpoons CO_2 + H_2 \qquad (1.6)$$

Furthermore, the reaction is normally conducted under pressure (in a range between 15 and 50 bar, depending on the temperature used) and, when purification of the produced hydrogen is needed, the process is favoured by the pressure condition: H_2 can be simply purified by adsorption or by using membrane technology, while CO_2 can be easily separated by carbon dioxide sequestration.

The importance of this reaction is given by the fact that hydrogen is expected to play a key role as energy carrier in future energy systems of the world, since it can be used either as a clean fuel or as raw material in a wide variety of industries (petrochemical, ammonia, methanol, metallurgical, etc.)[9].

1.3.5 Hydrodeoxygenation (HDO)

In the hydrodeoxygenation process, glycerol reacts with hydrogen to generate reduced products and water by a series of hydrogenation (C-O bond cleavage by H_2) and dehydration (C-O bond cleavage through removal of H_2O) reactions. Decarbonylation and decarboxylation can also be

used as processes to obtain the same target of products, but these imply cleavage of C-C bonds and subsequent reduction in carbon chain length, which is undesirable for value-added chemicals production. Indeed, the big advantage of HDO is that selective cleavage of C-O occurs, and products with the same carbon number of the original feedstock can be formed. The complete deoxygenation yields propane (as shown in ***Figure 8***), but it is also possible to stop the reaction earlier, and so, to obtain a pool of different functionalised products.

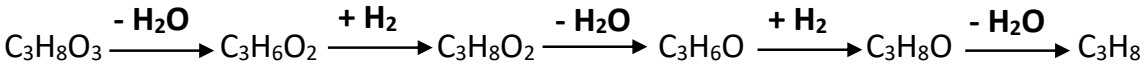

Figure 8. *Path during HDO of glycerol.*

Among them, from a commercial point of view, propylene glycol is again the most interesting one, as commodity chemical, together with the 1,3-propanediol, which can be used as monomer for the production of polyester fibres.

1.4 CHARATERISTICS OF AQUEOUS-PHASE REFORMING

Aqueous-Phase Reforming is only one of the different possible pathways for the thermochemical conversion of biomass-derived glycerol: steam reforming (SR), sorption enhanced steam reforming (SESR), supercritical water reforming (SCWR), partial oxidation (POR) and autothermal reforming (ATR) are all processes that lead to the same products. The major constituents of the gaseous mixture resulting from the thermochemical decomposition of glycerol are hydrogen, carbon monoxide, carbon dioxide and methane, while negligible amounts of compounds such as short chain alcohols (like methanol and ethanol), ethylene, acetaldehyde, acetic acid, acetone, acrolein and water are also formed[10,11]. The main glycerol reforming processes involve fixed bed reactors, at temperatures in the range of 300–900 °C[12], and usually the use of catalysts, necessary to lower the activation energy and to favour the kinetics of the reaction. To obtain a more productive and economically suitable reaction, the catalysts must be highly active and stable, generate the smallest amount of coke, be sintering-resistant, and not facilitate undesirable parallel reactions such as methanation or Fischer–Tropsch synthesis.

Steam reforming (SR) is the most extensively investigated production route to hydrogen: it involves adding glycerol and water to a reactor, where glycerol is gasified and water is turned into steam[13,14]. The advantage of the process is that the produced hydrogen can be simultaneously removed from water, increasing the yield of the reaction. On the other side, the overall SR process is endothermic, and the energy consumption to vaporize the reaction mixture is very high. Furthermore, the best results for glycerol SR process are obtained at temperatures between 525 – 725 °C, and the control under these conditions is difficult and expensive, because of the elevate energy consumption and the elevate cost of material for construction of the reactor[15,16,17].

A way to enhance the SR is to carry out the process in the presence of a CO_2 sorbent, in order to shift the equilibrium towards products. The sorbent improves the reforming by increasing the concentration of H_2, while reducing the concentrations of CO, CO_2 and CH_4, and subsequently increasing the H_2 yield. However, the problem of this so-called Sorbent Enhanced Steam Reforming (SESR) is that the CO_2 sorbent saturates itself as sorption proceeds with time, causing a loss of CO_2 capture capacity and, so, a loss of the improvement on the process. Thus, even if this process is able to generate high purity H_2 gas, the necessity of regenerating the sorbent constitute a big energy penalty[6].

Partial Oxidation Reforming (POR) occurs under atmospheric pressure and with quantities of oxygen below the stoichiometric ones, in order to avoid the complete combustion of the reactant[12,18,19]. This process is really promising in terms of temperature control and energy consumption, since it is energy self-sufficient and does not need any external power supply; oxygen provides itself the heat through the oxidation reaction. The efficiency of the exothermic process depends directly on controlling the amount of oxygen fed[20]. The issue with the POR is that, because it involves rapid consumption of oxygen and high temperatures, the process easily gives various parallel and undesired reactions.

Similar to POR, there is the Autothermal Reforming (ATR), which involves carrying out steam reforming in the presence of oxygen. The heat released by the oxidation of glycerol is used to sustain the steam reforming reaction, which is endothermic. When the oxygen fed is enough, the heat released by the oxidation is cancelled out by the heat consumed by the steam reforming: this condition, where no external heating is needed, can be defined as thermoneutral. The temperature at which thermoneutrality is reached is called adiabatic temperature. In the case of ATR, the disadvantage is constituted by the fact that the molar amount of H_2 formed for each

mole of glycerol is lower than the amount of H_2 formed for each mole of glycerol during SR, because of the oxidation process and the subsequent larger amount of CO and CO_2 produced.

Supercritical water gasification (SCWG) of glycerol stands out for operating with high pressures and low temperatures, in which water is above its critical point (374 °C, 218 atm), providing interesting properties like low viscosity, high diffusivity and low dielectric constant[21,22,23]. SCWR has attracted increasing interest thanks to its high efficiency and selectivity in H_2 production, due to the unique properties of supercritical water, that allow higher space-time yields and reduced mass transfer constraints. Furthermore, this hydrogen is produced under high pressure and can be therefore stored in cylinders[22], requiring little energy for its compression. In addition, many organic solvents and gases are completely miscible under these conditions, favouring a reaction environment with a single fluid phase[24,25]. The big disadvantages of the process, which make it not safe and not economically attractive[26], are given by the highly reactive environment, that causes corrosion on reactors and other equipment, and by the high pressures and temperatures required.

Aqueous-Phase Reforming (APR) is usually performed at high pressures and moderate temperatures (40 – 60 bar / 270 °C) in a continuous stream, transforming glycerol into aqueous phase without pre-vaporization. The reasons that make APR one of the most interesting biomass valorisation processes to be investigated are several. First of all, the low temperatures used to carry out the process benefit the hydrogen production on two aspects: first, the energy requirement is remarkably lowered; second, the undesirable products are reduced by both minimizing the temperature of glycerol thermochemical reactions and promoting the WGS[27,28,29,30]. Then, APR process takes place in liquid phase, indicating unnecessary to remove water from the biomass feedstock and reducing the cost during all the process[31]. Another advantage comes from its eco-sustainability, APR uses renewable biomass-derived chemicals as feedstock, takes reactions at mild conditions, and produces hydrogen and other renewable and nontoxic chemicals[32,33]. Besides, the reaction can be conducted in a single-step chemical reactor system, allowing simplified processing and low energy consumption[34].

The typical reaction conditions for the thermochemical conversion of biomass-derived feedstocks are all grouped and shown in ***Figure 9***, where they are also compared to the catalytic processing conditions of petroleum feedstocks. As can be seen, APR is located in the mildest T and P corner.

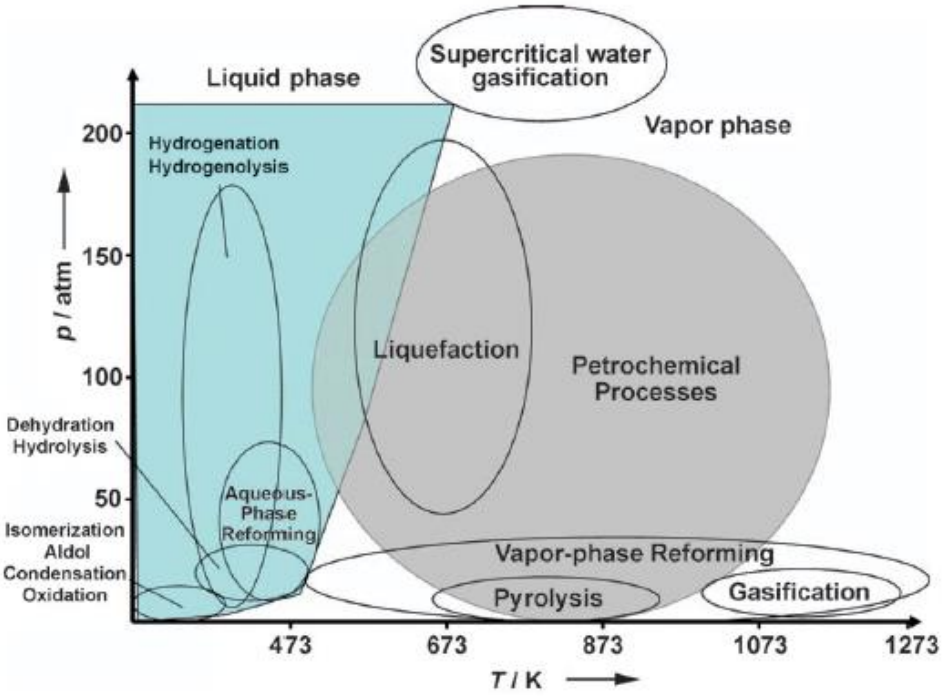

***Figure 9**. Diagram of approximate reaction conditions for the catalytic processing of petroleum versus biomass-derived carbohydrates*[35].

1.5 HYDRODEOXYGENATION (HDO)

The excess oxygen present in the biomass-based feedstocks can be removed basically through three different pathways: decarbonylation, decarboxylation or hydrodeoxygenation. Decarbonylation and decarboxylation imply the cleavage of C-C bonds, while the hydrodeoxygenation is more selective to the C-O bond scission. The advantages of the HDO over the other two reactions are numerous:

- It is more eco-friendly since, ideally, H_2O instead of CO_2 is produced with the oxygen elimination.
- It gives products in which the carbon chain length of the starting material is not varied, desirable to produce high added-values chemicals and fuels.
- It gives highly functionalised products, which are easy to transform into value-added chemicals.

HDO is basically a combination of the dehydration and hydrogenation reactions, where the substrate reacts with hydrogen to generate reduced products and water. Due to the high boiling point of the highly oxygenated biomass-derived molecules, their upgrading processes must be

conducted in liquid-phase, in order to be able to carry them out with relatively low temperatures. The substrates to be investigated in the aqueous phase HDO, until now, are phenols, guaiacol and furfural, while the literature on the HDO of polyols is still limited.

Hydrodeoxygenation of polyols can be focussed either on the production of fuel-grade alkanes or on the production of a pool of functionalized liquid products. For the first target, complete oxygen removal is necessary, while for the second, partial deoxygenation is required to keep some oxygenated functionalities. The removal of oxygen atoms from the reactants is basically due to an hydrogenolytic reaction which can, of course, only occur in the presence of a hydrogen source. Normally, this hydrogen is added from an external gas source, but the low solubility of H_2 in water makes necessary high-pressure conditions, which have a negative impact both on the safety and the economics of the process. Besides, HDO of polyols with high pressure external hydrogen gives a poor selectivity for liquid products, with significant formation of CH_4. In the light of all these disadvantages, to improve the process a novel approach of conducting the reaction without external H_2 is being investigated[36,37,38,39,40,41]. One of the most promising alternatives is to use hydrogen produced *in-situ*, that can be obtained in two different ways[42]:

- Catalytic Transfer Hydrogenation (CHT), that uses hydrogen donor molecules like either small alcohols (methanol, ethanol and propanol) or formic acid.
- Aqueous-Phase Reforming (APR), that produces H_2 by dehydrogenation of the substrate itself.

CTH reactions, using H-containing compounds as H-donors, spill active H species and make it react with the substrate instantaneously on the surface of the catalysts. The intrinsic rate of this approach to C-O cleavage is much higher than that of *in-situ* hydrogenolysis using the substrate itself as H-donor, but it also needs additional separation and recycling stream of the unconverted hydrogen donor from the reaction. In comparison, the big advantage of the second approach is that it can be carried out in one pot coupling the APR and the HDO in the same reactor. Basically, using the *in situ*-generated hydrogen by the reforming of part of the reactant, it is possible to obtain the liquid reduced products of HDO of the remaining polyol in a unique system. Furthermore, from the thermodynamical point of view, reforming is an endothermic process while hydrogenation and hydrogenolysis are exothermic reactions: therefore, the combination of them is considerable slightly exothermic, which makes the entire process energetically viable. In addition, processing into aqueous phase avoids the evaporation of huge

amounts of water, contributing to the energetic and economic favourability of the process. However, the use of water as solvent has rarely been done in industrial chemistry until now, and it requires to develop effective catalysts (both in hydrogen production and biomass-derived chemicals hydrodeoxygenation) resistant to the harsh conditions of hydrothermal reaction.

1.6 CATALYSTS CHARATERISTICS FOR APR AND HDO

1.6.1 Catalysts for APR

To produce hydrogen *in-situ*, Aqueous-Phase Reforming (APR) needs a catalyst that makes it possible to carry out the reaction at low temperatures. Moreover, to be effective, it also needs to have a good selectivity, otherwise the reaction of H_2 with CO and CO_2 (methanation reaction) would be highly favoured. A good catalyst, thus, must be more active towards the cleavage of C-C and C-H bonds rather than the C-O bonds, and should promote the removal of adsorbed CO by the Water-Gas Shift (WGS) reaction. Dumesic and co-workers were the first to develop APR of various biomass-derived compounds, and they reported that platinum, ruthenium and, in general, metals from Group VIII show a high APR activity[12,43,44]. Platinum catalysts supported on metal oxides (like Al_2O_3) are recognized as the most active and selective catalysts[45,46,47], due to their moderate activity in C-C and C-H bond cleavage[48] and low methanation and Fischer-Tropsch activity. To have even higher activity and selectivity in hydrogen production, bimetallic Pt-based catalysts are also being investigated. The strong binding on the platinum surface of hydrogen and carbon monoxide products, together with the oxygen intermediates, negatively affects the catalyst reactivity as a result of the blockage of the active sites[49]. Thus, the use of lower amounts of Pt and the addition of other active metals decrease the adsorption strength of H_2 and CO, lowering the blockage of the active sites, and improving this way the catalytic reactivity.

1.6.2.1 Use of Ni in APR catalysis

The problem with the catalysts based on noble metals is that, unfortunately, they have huge limitations imposed by availability and costs. For this reason, it has been necessary to investigate for substituents like transition metals. Davda et al. found that the reaction rates decrease in order of Pt ≈ Ni > Ru > Rh ≈ Pd > Ir at temperatures from 210 to 225 °C[50]. Therefore, nickel-based catalysts represent a valid alternative to the Pt-based ones because of their economic advantages and the good intrinsic activity in C-C scission[51,52,53]. These kinds of

systems, supported on conventional alumina, showed good mechanical strength and optimal textural properties, like high superficial area and porosity. They have been so extensively investigated, but, under APR hydrothermal conditions, Al_2O_3 can be easily hydrated and transformed into boehmite (AlOOH), causing significant changes in surficial area and acidity. These alterations may be the reason of dissolution of the support and oxidation and sinterisation of the metal particles (the active part of the system), and finally provoke the activity decay. In the light of this, it is important to work on the nature of the support, which has a main role in the catalysts activity[54,55], in order to develop more efficient nickel-based systems.

Nickel aluminate spinel ($NiAl_2O_4$) can represent a good option due to the good textural, redox and acid-base properties, the high thermal stability, and the strong mechanical strength[56]. Nickel aluminate spinels are a typical example of oxide spinels, a group of compounds with the general formula AB_2O_4, where either A is the divalent cation (Ni^{2+}) and B the trivalent one (Al^{3+}), and they occupy two different kinds of crystallographic sites, one of which is tetrahedrally co-ordinated by the anions and the other is octahedrally co-ordinated. Per unit cell of four O^{2-} anions, there are two octahedral sites and a tetrahedral one, and, in many cases, the single Ni^{2+} cation occupies the tetrahedral site, while the two Al^{3+} cations occupy the other two. The structure of a spinel with the general formula of AB_2O_4 is reported in ***Figure 10***.

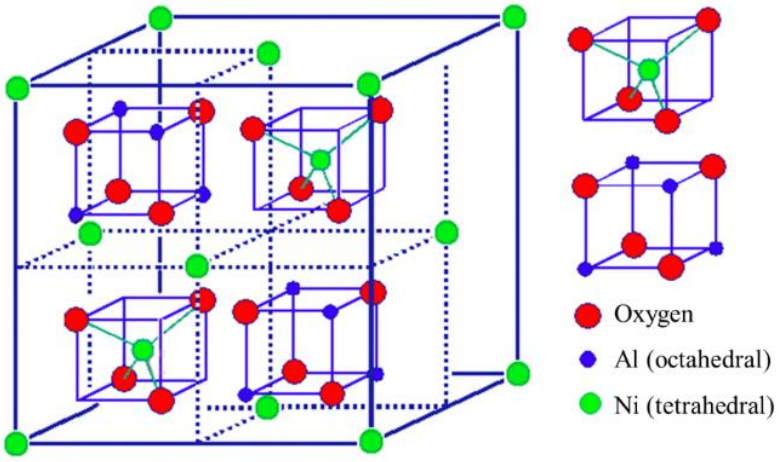

Figure 10. *Crystal structure of a spinel type AB_2O_4.*

The catalytic site required by the H_2 production is a metallic one, and it is so necessary to reduce the $NiAl_2O_4$ spinel precursor to obtain metallic Ni^0, thus, the catalytic activity. The rest of the structure is transformed into γ-Al_2O_3, which in this case is less subjected to transformations

since it remains in the core of the structure and is protected by the metallic nickel layer. The reducibility of these catalysts has been extensively studied and, based on the reduction temperature, different nickel species can be found[57]. To obtain Ni^0 starting from the Ni^{2+} forming the spinel, the reduction temperatures must be between 600 °C and 1000 °C. At these temperatures, relatively small metallic Ni crystallites with a good textural stability and in strong interaction with alumina are formed, and this implies an important advantage for the catalytic activity because of a better stability provided to the system. Furthermore, when the spinel is reduced, the oxygen vacancies move through the inner part of the particle to the surface and, as a consequence, changes in the surface microstructure occur with a major fraction of nickel metal particles forming on the surface. In addition, the consequent layer of nickel aluminate in between the alumina and the metallic nickel particles can prevent sinterisation, and so, the deactivation process of the system, making it way more stable.

1.6.2 Catalysts for APHDO

To make the Aqueous-Phase Hydrodeoxygenation (APHDO) possible, the catalysts need to have different catalytic sites. APHDO involves, first, APR reaction for the *in-situ* hydrogen production, then, a combination of several other reactions, such as hydrogenation, hydrogenolysis, decarbonylation and dehydration. Some of them are favoured by metallic sites, while the others, by acidic sites, for this reason, bifunctional catalysts are being investigated. The acid function should ensure the adsorption and activation sites for the oxygen from the O-containing compounds. Subsequently, the activated O-containing compounds should be hydrogenolysed by the hydrogen, activated thanks to the metallic sites. A wide variety of products can be generated by this pathway, depending on the substrate and the relative rates of C-C vs. C-O bonds scission, but in general, products with a minimum loss of carbon in the chain are desired, so, the catalysts must offer selectivity to C-O cleavage with respect of C-C. As metal sites, besides catalysing APR reaction, also catalyse C-C scission, in order to favour the C-O scission, the acid function must be properly tuned. This tuning can be achieved by two different approaches:

- Promotion of acidity with oxophilic oxides (oxides of Re, W, Mo, Nb, etc.)
- Employ of acid supports (SiO_2-Al_2O_3, ZSM-5, etc.)

Depending on the type of acidity (Lewis or Brønsted), the final products distribution can change. For example, while Lewis acidic sites eliminate the primary hydroxyl groups of a molecule, secondary hydroxyls are more prone to be removed as water on Brønsted acid sites.

According to ***Figure 11***, two main pathways occur in the APHDO in the presence of a bi-functional catalyst: dehydrogenation of the substrate in metallic sites, that generates H_2, and a series of dehydrations/hydrogenations in acid sites.

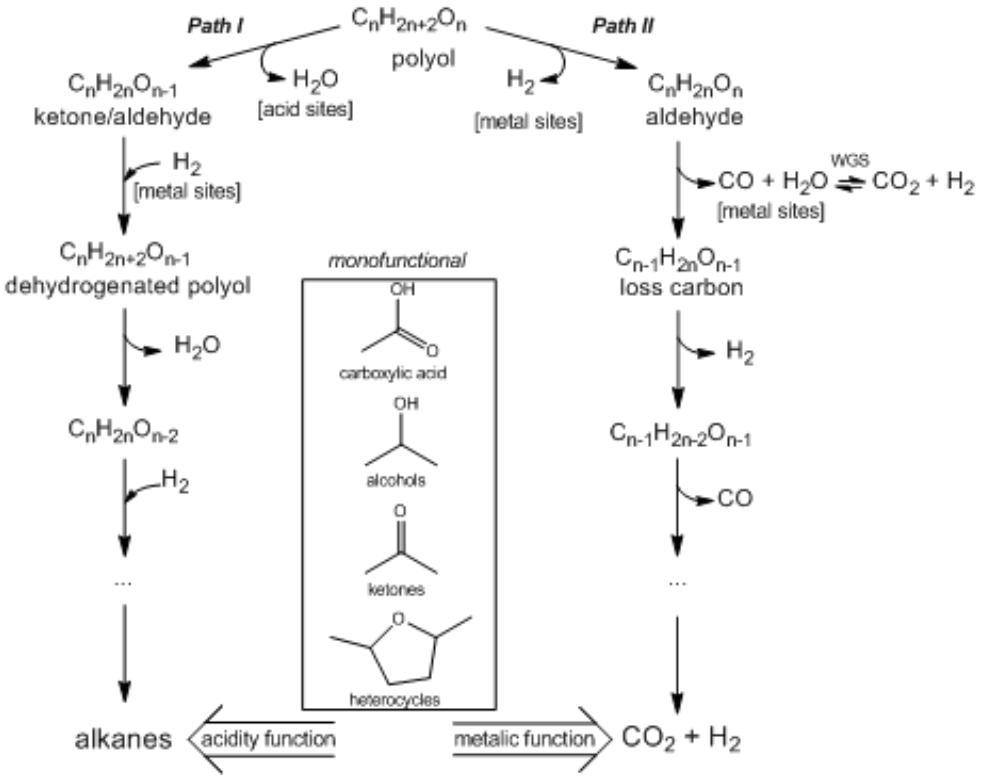

Figure 11. *Generic paths during aqueous phase HDO of polyols.*

The former path consists in consecutive C-C scissions and dehydrogenation reactions, leading to products with a shorter carbon chain. This path should be favoured when the target is the hydrogen production, indeed, further H_2 can also be produced by WGS reaction of CO from decabonylation. On the other hand, when the target is the production of monofunctional chemicals or alkanes, the latter path is to be favoured. It consists in the dehydration of the substrate and in the subsequent hydrogenation, which gives products with less hydroxyl groups than the starting material. The intermediate products can undergo further dehydration/hydrogenation, until the complete deoxygenation and the alkanes formation.

To conclude, tuning the catalysts functionalities (acid/metal) properly, besides optimizing the reaction conditions, HDO can be focused into the different strategies, depending on the desired product (light alkanes, hydrogen or monofunctional compounds).

1.7 HDO OF GLYRECOL

Hydrodeoxygenation of glycerol can give a big variety of products. Several reaction mechanisms have been proposed in literature, but two of them revealed themselves to be the most common[58]:

- Dehydration/hydrogenation route,
- Dehydrogenation-dehydration-hydrogenation route.

Specifically, in the case of Aqueous-Phase Hydrodeoxygenation of glycerol, where part of the reactant is used for hydrogen formation, the reaction is reported to follow both the former and the latter mechanism, with the dehydration/hydrogenation one more commonly accepted[39]. According to this route, glycerol is first dehydrated to hydroxtacetone which then hydrogenates to 1,2-propanediol. Apart from these two chemicals, other stemming common products are 1,3-propanediol, propanols and degradation products, like ethylene glycol, methanol, and ethanol. 1,3-propanediol is formed from dehydration of glycerol to 3-hydroxyprpionaldehyde and subsequent hydrogenation. Propanols are formed via further hydrogenolysis of both propanediols. Ethylene glycol and methanol are formed via direct C-C cleavage of glycerol, while ethanol is proposed to be formed either via further hydrogenolysis of ethylene glycol or via degradation reaction of 1,2-propanediol. A scheme of the possible reaction pathways is reported in ***Figure 12***.

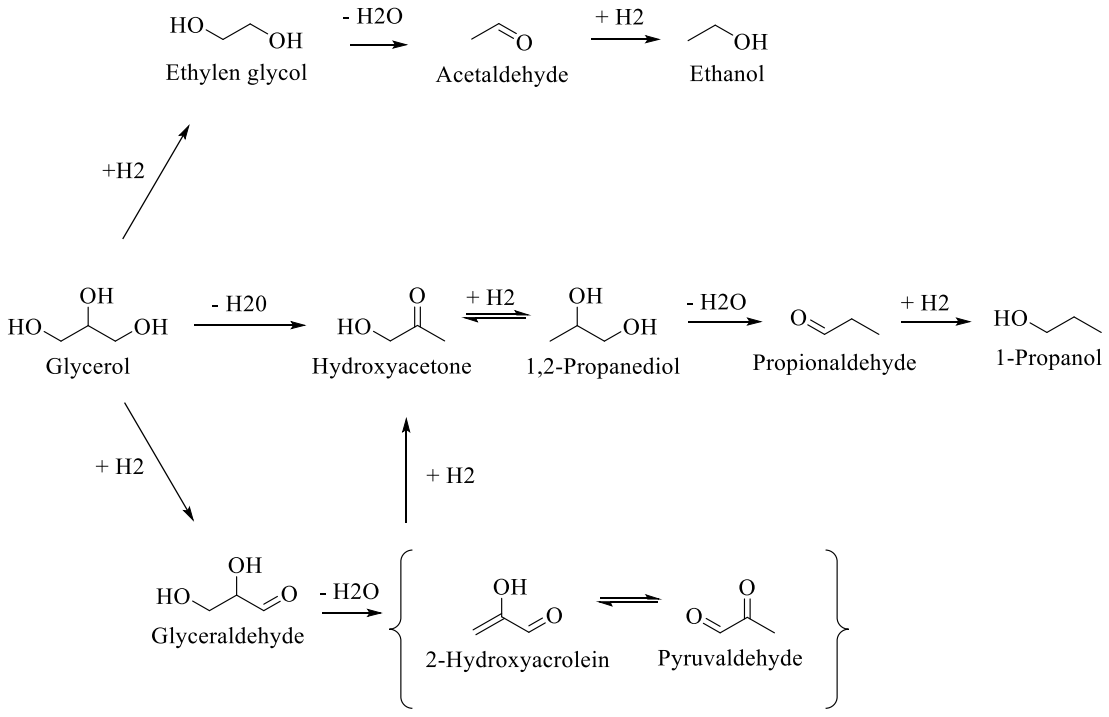

Figure 12*. Glycerol HDO reaction pathways.*

A variety of catalysts has been investigated and, as widely discussed in the previous section, it is active both in glycerol APR and HDO and so presents both metallic and acid catalytic sites. Pt-based catalysts showed a good activity. According to Wawrzetz et al.[59] over Pt/Al_2O_3 catalyst, glycerol dehydrogenates to H_2 and CO_2, and part of the formed H_2 is consumed during the propylene glycol that proceeds via dehydration/hydrogenation route. Pt is able to catalyse dehydrogenation and hydrogenation reactions, while dehydration occurs on the support with the help of the platinum. Liu et al.[60] proposed that over a $Pt\text{-}Ir\text{-}ReO_x/SiO_2$ catalyst, the first step of glycerol conversion could be either dehydrogenation or dehydration of the reactant to glyceraldehyde and hydroxyacetone, respectively, and then further dehydrogenation/dehydration occur. In addition, always in order to avoid the use of Pt, also other systems have been explored, which included metals active in APR (such as Ni, Ru, Rh, Pd, Ir, etc.) and different kinds of acid supports and oxophilic metals (live oxides of Re, W, Mo, Nb, etc.). Gandarias et al.[61,40] conducted tests over monometallic and bimetallic $Ni\text{-}Cu/Al_2O_3$ catalysts, concluding that glycerol HDO mechanism varies depending on the origin of the active hydrogen species (which can be the H_2 produced via glycerol APR or the H_2 provided by an alcohol intermediate). Other studies have been conducted on a Pd/Fe_xO_y system[62], where the Pd is able to adsorb the hydrogen while the support to catalyse the dehydration, and on a Cu-Mg-Al catalyst[63], where the glycerol dehydration to hydroxyacetone proceeds on basic sites of the catalyst, and Cu sites serve as active site for both subsequent hydrogenation step of propylene glycol and formation of active hydrogen atoms.

2. AIM OF THE THESIS

Nowadays, petroleum refineries are the main responsible of the production of a huge fraction of fuels and chemicals starting from oil and gas feedstocks. Due to the decrease of fossil reserves, so their uncertain availability, and the on-going price increase, together with environmental concerns, society is becoming aware of the need for alternatives. Use of biomass as feedstock can help these needs: it is a renewable source, almost all the products made out from fossil fuels can also be obtained starting from it, and the impacting emissions of Green House Gases produced during the valorising processes are lower. Among all the compounds constituting biomass, feedstock for the Green Chemistry, glycerol is one of the most relevant: this molecule, thanks to its high functionalization, can easily and variously be valorised and recycled into high value-added products.

Glycerol hydrodeoxygenation process brings to the production of various liquid products, like hydroxyacetone, ethylene glycol and propylene glycol, which are interesting chemicals with a wide range of applications in pharmaceuticals, cosmetics, polymeric resins, food and tobacco industries, and so on. Most of the studies on this reaction have been carried out under hydrogen pressure providing H_2 from an external source. The need of external supply, and the requirement of high pressures, in combination with hydrogen's properties (like high flammability and diffusivity), represent a big disadvantage of this method, having a negative impact not only on the environment, but also on the process economics. To overcome these issues, a promising and alternative approach, which is being studied in the recent years, is to use hydrogen produced *in-situ* via Aqueous-Phase Reforming (APR) of part of the glycerol to carry out the HDO of the remaining part.

The catalytic systems needed for this process must be active in different reactions (such as hydrogenation, hydrogenolysis, decarbonylation and dehydration) which occur at different catalytic sites, for this reason, bifunctional catalysts, that present metallic and acid sites, seem to show a good activity. Nickel aluminate spinel have been found to be promising precursors of Ni-based catalysts for APR reaction, with high conversion of glycerol and hydrogen production. In order to enhance the HDO activity, and therefore the amount of liquid oxygenated products obtained, this thesis work was focused on providing the acid function to the nickel aluminate catalyst through doping with an oxophilic metal, tungsten (W), and studying the effect. Then, the effect of synthesis method was also studied and, finally, the Weight Hourly Space Velocity (WHSV) was evaluated.

To have, in the end, a general picture of the effects of dopant content, synthesis method and WHSV on the catalytic system, several and more specific goals were reached:

- ✓ Synthesis of pure nickel aluminate spinel ($NiAl_2O_4$) by using sol-gel method.
- ✓ Synthesis of W-doped catalysts, by sol-gel method, using different amounts of W (1, 3, 5 and 9 wt. %).
- ✓ Characterization of all the synthesised catalysts to study the physicochemical properties, and then, to find the correlation with their catalytic activity.
- ✓ Evaluation of the catalytic activity in glycerol HDO, in a continuous tubular reactor, and finding the correlation between the performance of the systems and the tungsten content.
- ✓ Evaluation of the effect of the synthesis method. To do this, another catalyst with 1 wt.% W was synthesized via the impregnation method.
- ✓ Study of the effect of Weight Hourly Space Velocity (WHSV) by changing the feeding flow of glycerol (in particular, doubling it).

3. MATERIALS & METHODS

Materials, equipment and experimental methods used for developing this work are explained in this chapter.

Firstly, the reactants and the preparation methods used in catalysts synthesis are listed and explained. Secondly, the methodology used for catalysts' characterization is specified. Then, the equipment used for catalytic activity evaluation, with details of the employed operating conditions, is described. Finally, the analysis system for determining and quantifying effectively and accurately the composition of the reaction products is described, together with the definition of reaction indices and their calculations.

3.1 MATERIALS

In order to synthetize and characterize the catalysts, and then, to carry out the reaction and analyse the obtained products, the following reactants have been used.

For the sol-gel synthesis of the solids: Nickel nitrate hexahydrate $Ni(NO_3)_2 \cdot 6H_2O$ (Alfa Aesar, Ni 19.8% min.), Aluminium nitrate nonahydrate $Al(NO_3)_3 \cdot 9H_2O$ (Merck, 100 % for analysis), Ammonium metatungstate hydrate $(NH_4)_6H_2W_{12}O_{40} \cdot xH_2O$ (SigmaAldrich, 99.99%), anhydrous Citric acid $C_6H_8O_7$ (Sigma Aldrich, 99.5-100.5%), deionized water.

For characterization and catalytic activity evaluation: Synthetic Air (Air Liquide), Hydrogen H_2 (Air Liquide, 5.0), Argon Ar (Air Liquide, 5.0), Helium He (Praxair, 5.0), Nitrogen N_2 (Praxair, 5.0), Hydrogen/Argon mixture 5%H_2-Ar (Praxair), Ammonia/Helium mixture 10%NH_3-He (Praxair), Oxygen O_2 (Praxair, 5.0).

For the catalytic tests: Glycerol $C_3H_8O_3$ (Panreac, 99.5%), deionized water.

3.2 CATALYSTS SYNTHESIS

3.2.1 Thermogravimetric analysis

To evaluate the unknown hydration degree of ammonium metatungstate, a thermogravimetric analysis (TGA) was conducted. TGA is a technique in which the mass of a substance is monitored as a function of temperature or time as the sample specimen is subjected to a controlled temperature program in a controlled atmosphere. A Setaram Setsys Evolution

thermobalance, equipped with cylindrical graphite furnace and PID integrated temperature control, was used. About 50 mg of the sample were placed in a corundum crucible, and subsequently, the sample assay was performed with a constant heating rate of 10 °C/min from room temperature up to 200 °C, in an air flow of 50 cm^3/min.

3.2.2 Catalysts synthesis by sol-gel methods

Sol–gel method is used for the preparation of inorganic polymers or ceramics, through a transformation from liquid precursors to a sol and finally to a gel. The gel structure is generally defined as a non-fluid 3D network that extends through a fluid phase. The sol-gel chemistry is centred on the ability to produce a solid-state material from a chemically homogeneous precursor. Thanks to the homogeneity of the precursor and so, to the absence of mass transport which can limit the reaction, the synthesis can be carried out at low temperatures and short times[64]. Sol–gel chemistry also enables a good control over particle morphology and size.

Specifically, among all the possible sol-gel methods, the citric acid sol–gel, also known as citrate sol-gel, is commonly used for the synthesis of metal oxide powders. In a typical synthesis carried out with this technique, aqueous metal salts are mixed with citric acid (a weak triprotic acid that is also an effective chelating agent)[65] and the resulting solution, when heated, forms a viscous solution or a gel. In an aqueous solution of metal ions of charge z^+, water molecules coordinate the metal via electrons in their bonding orbitals, and the result is a weakening of the O–H bonds of bound water molecules and, depending on the pH, deprotonation or hydrolysis occur. Thus, the function of the citric acid is to change the hydrolysis equilibria of dissolved metals, thanks to its chelating capacity, and to form stable aqueous metal complexes and structures that more closely resemble ‘gels’, as shown in ***Figure 13***.

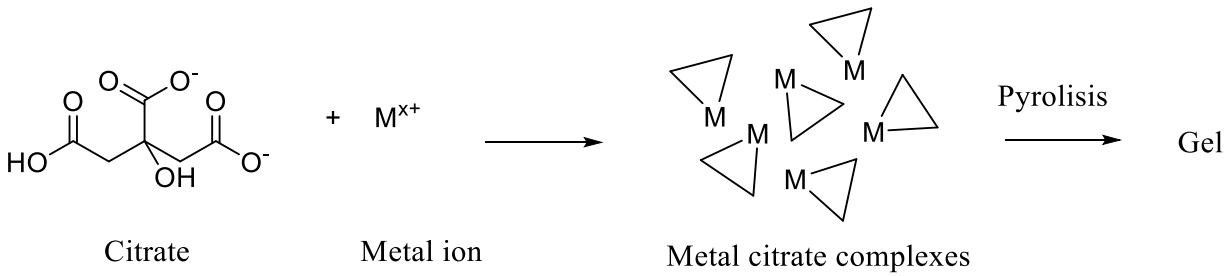

Figure 13. *Scheme of the citrate function.*

In addition, the presence of the organic matrix during the first stages of synthesis can ensure that, when nucleation occurs, the sites are evenly dispersed and numerous, promoting a small crystallite size. Moreover, in the case of ternary or quaternary systems, the matrix also ensures that the different metals remain mixed on an atomic scale. Subsequently, conversion of the gel to metal oxide is simply achieved by pyrolysis in air, with the maximum temperature depending on the specific system[66].

In this work, the citrate sol-gel method was used to synthesise different WNiAl ternary oxides with different amounts of tungsten (0 wt. %, 1 wt. %, 3 wt. %, 5 wt. % and 9 wt. %). The aim was to evaluate the effect of doping with tungsten on the catalytic activity of nickel aluminates spinel. The synthesis was carried out using nickel nitrate hexahydrate, aluminium nitrate nonahydrate and ammonium metatungstate hydrate as precursor salts of the metals, and citric acid as gelator agent.

For the synthesis of these WNiAl oxides, aqueous solutions of Ni^{2+}, Al^{3+} and W^{6+} salts and of the gelator agent were prepared, by simply adding deionized water to each precursor in separated beakers and subjecting them to magnetic stirring, in order to help the dissolution. The amount of water utilized to dissolve the reactants was the minimum necessary to have complete dissolution. The calculations for the metal precursors quantities were done considering the stoichiometric molar ratio Ni/Al of the spinel (1:2) and the nominal tungsten loadings, while the quantity of citric acid was calculated with the following equation (*3.1*):

$$R_{c/m} = \frac{mol_{CA}}{mol_m} = 1{,}2 \qquad (3.1)$$

where mol_{CA} is the number of moles of citric acid, while mol_m is the number of the total moles of metals (Ni + Al + W) in the solution. Once the metal precursors were completely dissolved, all their solutions were put together into a bigger beaker. Then, the solution of citric acid (again prepared with the minimum quantity of necessary water) was added dropwise, thanks to a peristaltic pump with a flow rate of 10 mL/min, while stirring. When the addition of the gelator agent was finished, the solution was further left under magnetic stirring, at room temperature, for 1 h. Subsequently, the temperature was raised up to 90 °C and kept until the gel formation, that occurred after about 4 h. After the gelation, the calcination step was needed. The final gel was transferred to a crucible and then introduced into a muffle where was subjected to a temperature ramp: firstly, the temperature was raised up from 25 °C to 850 °C with a rate of 2 °C/min, and secondly, it was kept at 850 °C for 4 h (in order to form spinel phase) and, finally, it was cooled down as quickly as possible to room temperature (to avoid phase transformation

or grain growth during conventional cooling rate, assuring at room temperature the crystalline structure exhibited by powder at high temperature). In the end, teal-coloured powder was obtained. The prepared solids were denominated x-WNiAl, where x represents the W loading in wt. %.

A pictorial scheme of the process for obtaining solids by sol-gel is presented in ***Figure 14***.

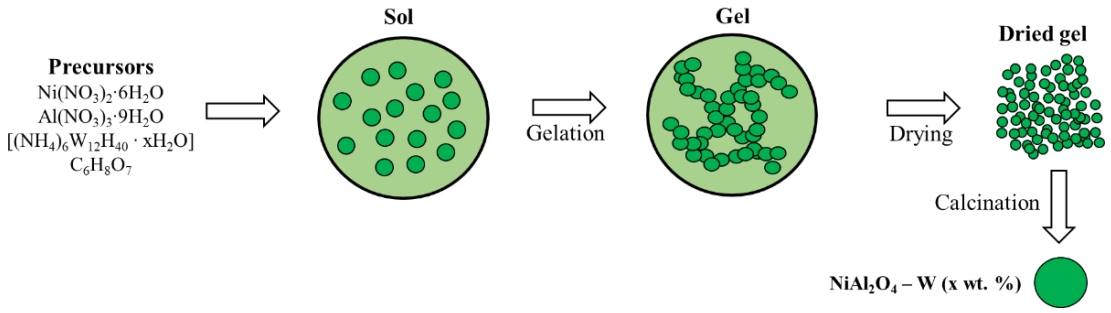

Figure 14. *Sol-gel synthesis of $NiAl_2O_4$ doped with W.*

3.2.3 Catalysts synthesis by impregnation

After the catalytic studies on glycerol HDO over the catalysts synthetised via sol-gel, it was decided to synthesize the catalyst formulation showing the best performance with another synthesis method, aiming to investigate a possible effect of the synthesis method on the catalytic activity.

The catalyst to be synthetised via impregnation was the one with the minimum tungsten loading (1 wt. %), which showed a good compromise between glycerol conversion and selectivity towards the major products.

Pure stoichiometric nickel aluminate spinel ($NiAl_2O_4$) was synthesized using the same sol-gel procedure previously specified. The addition of tungsten was carried out in a second moment using a rotavapor and a burette connected to it. The desired amount of this pure $NiAl_2O_4$ was put in the round-bottomed flask of the rotavapor, and afterwards, the flask was put in the 40 °C water bath with a moderate rotation speed. An aqueous solution of tungsten precursor (the same as for sol-gel synthesis) was added dropwise thanks to a burette connected to the system. When all the water added to the system was evaporated, the flask was taken from the rotavapor and put in an oven, at 90 °C for a couple hours, in order to assure the complete dryness of the sample. When the content of the flask was completely dried, it was put in a crucible and then

in a muffle for the calcination step. The temperature ramp at which the solid was subjected to was different this time: firstly, the temperature was raised up from 25 °C to 100 °C with a rate of 2 °C/min, secondly, it was kept at 100 °C for 1 h. This sequence was done to dry the solid. Then, the temperature was raised up again to 400 °C with a rate of 2 °C/min and, finally, this condition was kept stable for 2 h. The cooling down step was again programmed to be as rapid as possible. The product obtained in the end presented itself as a teal-coloured powder, identical to the solids previously synthesised. The prepared solid, this time, was denominated 1W/NiAl.

3.3 CHARACTERIZATION TECHNIQUES

Several characterization techniques were used on the fresh catalysts with the purpose of determining their physicochemical properties and establishing, in a second moment, the relationship between the catalysts structure and their activity.

The principles of the techniques and the equipment and protocols applied are described in this section.

Certain characterization techniques could be carried out on the catalyst precursors as such, thanks to an *in-situ* reduction, while other techniques required a prior *ex-situ* treatment to allow the investigation on the properties of the effective catalysts. For this reason, about 1 g of each sample was reduced *ex-situ* in a tubular quartz reactor, at 700 °C, for 1 h (heating rate 5 °C/min), into a flow of 10 mL/min of H_2 and 60 mL/min of N_2. Afterwards, the system was cooled down into a flow of 60 mL/min of N_2. With the help of liquid nitrogen, during the cooling down step, the sample could reach temperatures around 10 °C and, under these conditions, an exothermic passivation process could be done, in order to stabilize the reduced product and avoid a deeper oxidation. For the passivation step the samples were kept into a flow of 10 mL/min of O_2 and 60 mL/min of N_2 for 10 minutes.

3.3.1 X-Ray Power Diffraction (XRD)

X-Ray Diffraction (XRD) is a fast analytical technique widely used for phase identification of crystalline materials. XRD is based on the interaction between crystalline samples and monochromatic X-rays; when the conditions satisfy Bragg's Law (*3.2*), this interaction is able to produce constructive interferences and a diffracted ray.

$$n\lambda = 2d \cdot sin\theta \qquad (3.2)$$

In this equation, *n* is an integer determined by the given order, λ is the wavelength of the X-ray, *d* is the space between the planes in the atomic lattice, and θ is the angle between the incident ray and the scattering planes.

X-rays are generated by a cathode ray tube, filtered to have a monochromatic radiation, collimated to concentrate, and finally directed to the previously grounded and homogenized samples. With these powder-form samples, all the possible orientations are represented on the surface and therefore exposed to the X-ray beam. As the samples rotate, they give different incidence angles θ, while the detector rotates with a double angle (2θ), picking up a continuous radiation background with a series of maxima, corresponding to the diffracted X-rays. The spectrum this way obtained is called *diffractogram*, whose positions 2θ and intensities are characteristic of each crystalline phase. The identification of the crystalline phases is done by comparing the experimental diffractogram with those of each phase collected in a database called PDF (Powder Diffraction File) established by the ICDD (International Center for Diffraction Data).

With the information on a diffractogram, applying the Scherrer's equation (*3.3*), it is then possible to calculate the size of the crystallite of the identified phase.

$$\tau = \frac{K\,\lambda}{\beta \cdot \cos\theta} \qquad (3.3)$$

where τ is the mean diameter of the crystalline domain (in Å), θ is the Bragg angle (in degrees), K is the dimensionless shape factor (0,89 for spheric crystals), λ is the wavelength, and β is the line broadening at half the maximum intensity (FWHM), in radians, calculated by the Warren's equation (*3.4*):

$$\beta = \sqrt{\beta_{exp}^2 - \beta_i^2} \qquad (3.4)$$

where β_{exp} is the experimental width and β_i is a correction due to the device.
The determination of the FWHM has been done by processing the diffractograms with the interface WinPLOTR from Fullprof suite software.

Applying the Bragg's Law on the diffractogram, it is also possible to calculate the lattice parameter, which refers to the physical dimension of unit cell in a crystal lattice. For cubic systems, the equation is the following (*3.5*)

$$a = \frac{\lambda}{2sin\theta}\sqrt{h^2 + k^2 + l^2} \qquad (3.5)$$

being *h, k,* and *l* the Miller indices, which indicate the orientation of a plane or set of parallel planes of atoms in a crystal.

Experimental procedure

XRD measurements were carried out in a PANalytical Xpert PRO model diffractometer with graphite secondary monochromator and PixCel detector, vertical goniometer (Bragg-Brentano geometry), operating with $Cu_{K\alpha}$ (1.541874 Å). Each sample was scanned from 10 to 80° (2θ) and a continuing time of 2 s. The equipment was controlled with the PANalytical Xpert HighScore Data Collector software. Analysis and identification of phases have been carried out at Advanced Research Facilities (in advance SGIker) of the University of the Basque Country (UPV/EHU).

3.3.2 X-Ray Fluorescence (XRF)

X-Ray Fluorescence (XRF) is a non-destructive analytical technique used for determining the elemental composition of solid and liquid samples. XRF analysis can determine the composition of a sample by measuring the fluorescent (or secondary) X-rays emitted from the sample when it is excited by a primary X-ray source. Each of the elements present in the sample produces a set of characteristic fluorescent X-rays, a "fingerprint", which is unique for that specific element because of the wavelengths λ, and with an intensity that depends on the concentration. The analysis can be performed sequentially, measuring the intensity of X-rays at different wavelengths one after another, or simultaneously, when at fixed positions the intensities of X-rays at different wavelengths are measured at the same time.

Experimental procedure

The analyses were carried out in a PANalytical AXIOS model sequential XRF spectrometer equipped with a rhodium tube, three detectors (gas flow, scintillation and Xe sailing) and a maximum power of 4kW (SGIker facility). The crystal bead was prepared by melting a mixture of the flux in an induction micro-furnace, Spectromelt A12 (from Merck, chemical composition: 66% dilithium tetraborate, 34% lithium metaborate), with the sample dried and grounded in proportions of approximately 20:1. Well-characterized international rock and mineral standards were used for calibration.

3.3.3 Temperature Programmed Reduction (H_2-TPR)

Temperature Programmed Reduction (TPR) is widely used in catalysis when the material that must be characterized is susceptible to reduction by a diluted gas. The solid sample is submitted

to a programmed temperature ramp while a reducing gas mixture is flowed over it; in this way, while the temperature increases, the solid is reduced. The most used reducing agent, due to its simplicity and to its high reducing power, is H_2. During the analysis, the concentration of H_2 in the exhaust stream is usually measured by a previously calibrated TCD (Thermal Conductivity Detector). The integration of released H_2 flow versus time reveals the capacity of reduction of the solid (reducibility), and the temperature at which the reduction takes place reflects the ability to reduce the sample.

Experimental procedure

The H_2-TPR analysis were carried out in a Micrometrics AutoChem 2920 apparatus. About 40 mg of sample were placed in a U-shaped quartz reactor and were initially flushed in an He stream, at 550 °C (heating rate 10 °C/min). After 1 h at that temperature, the sample was cooled in an Ar stream to room temperature. At this time, a freezing mixture (isopropanol/liquid nitrogen) was placed to trap the water that might be generated in the reduction of an oxide and may disturb the TCD performance. Finally, a 5%H_2-Ar flow was passed through the sample while the temperature was increased up to 950 °C (heating rate 10 °C/min) and held for 1 h.

3.3.4 Temperature Programmed Desorption (NH_3-TPD)

Temperature Programmed Desorption (TPD) is used for understanding surface-acid-sites-catalysed reactions on oxide catalysts and for determining the density of the acid sites. The technique is based on the chemisorption of a gas on a solid, and its subsequent desorption due to a progressive temperature increase. NH_3-TPD is typically used to determine the total acidity of a solid surface, since ammonia is a thermally stable molecule, with a pKa =9.27 and a small diameter, that make it theoretically accessible to all acid sites, from the weakest to the strongest. The obtained peak temperature and the peak area provide information, respectively, about the strength and the amount of the gas chemisorbed. No information about the nature of these acidic sites (Lewis or Brønsted) is obtained.

Experimental procedure

The total acidity of the reduced samples was evaluated by means of NH_3 adsorption pulses and the acid strength distribution by the subsequent temperature programmed desorption. Experiments were carried out in a Micrometric AutoChem 2920 and previously calibrated TCD detector. About 100 mg of sample were placed in a U-shaped quartz reactor and were initially pre-treated in a He stream, at 550 °C (heating rate 10 °C/min). After 1 h, the sample was cooled

at room temperature in an Ar stream. Then, the reduction was conducted at 700 °C (simulating the catalyst state at the beginning of HDO reaction) in 5% H_2-Ar flow (heating rate 10 °C/min), held for 2 h, and cooled down again at room temperature in an He stream. Afterwards, a series of 10% NH_3-He pulses were introduced at 90 °C. Subsequently, in order to remove the reversibly and physically bound NH_3 from the solid surface, the sample was exposed to an He flow, for 1 h, at the same temperature of the adsorption stage. Finally, the temperature was raised up to 950 °C (heating rate 5 °C/min) and the resultant signal was followed by TCD. The total acidity of the samples was calculated from the integration of the pulse peaks.

3.3.5 Nitrogen adsorption/desorption at -196°C

Nitrogen physisorption is a method used to investigate the textural properties of solids, as the adsorption-desorption of N_2 isotherms provide information on surface area and pore structure. It is a static method in which solid samples subjected to an adsorbate gas pressure reach an equilibrium. The physisorption phenomenon consists in the onset of low energy forces (Van der Waals forces) consequently to a contact between the adsorbate gas and the surface of the solid. When the temperature is low, the tendency of the gas is to form a monolayer on the solid surface, which depends exclusively on the size of the molecules. This way, simply by measuring the number of adsorbed gas molecules necessary to form this layer, the surficial area of the solid can be calculated. The most used adsorbate gas is N_2 that, at a temperature of -196°C, has a cross-sectional area of 0.162 nm^2. This phenomenon is easily described by an isotherm representing, at the given temperature, the amount of adsorbed gas at equilibrium as a function of relative pressure. All the isotherms obtainable trough this analysis, and recognized by the IUPAC, are shown in ***Figure 15***.

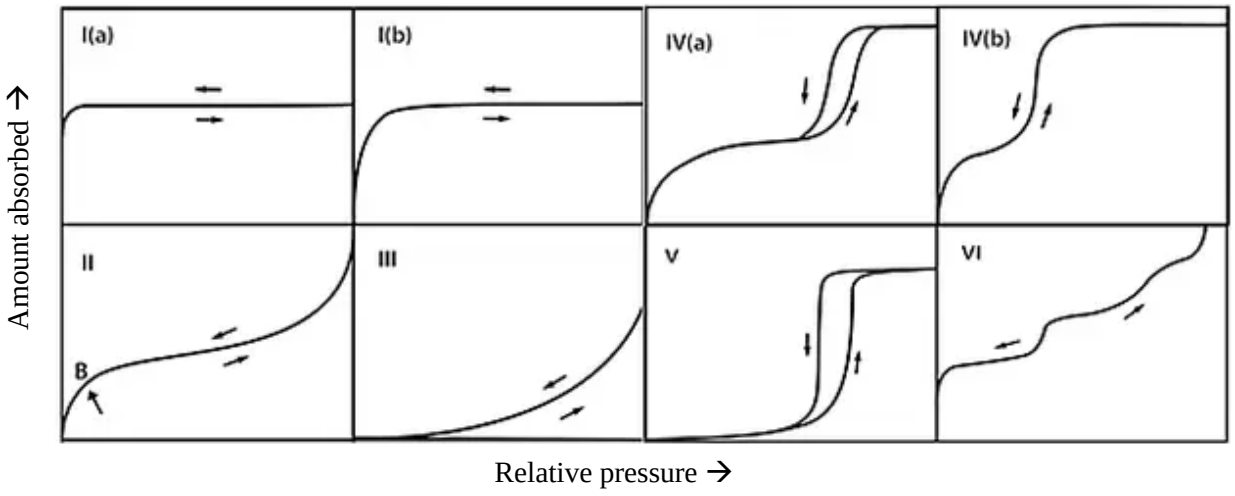

Figure 15. *IUPAC classification of adsorption isotherms*[67].

Plotting the total adsorbed and desorbed volume of gas at different equilibrium pressures, the corresponding desorption curves are obtained and information about the solid porosity are provided. In particular, on type IV(a) and V isotherms, it is possible to highlight the hysteresis phenomenon: this occurs when the pore width exceeds a certain critical width, dependent on the adsorption system and temperature (e.g., for nitrogen adsorption in cylindrical pores at -196 °C, hysteresis starts to occur for pores wider than ~ 4 nm)[68,69]. Different kinds of hysteresis are possible, and each type is closely related to particular features of the pore structure. The main types are reported in ***Figure 16***, they were identified in the original IUPAC classification of 1985 and it is now extended in the light of more recent findings.

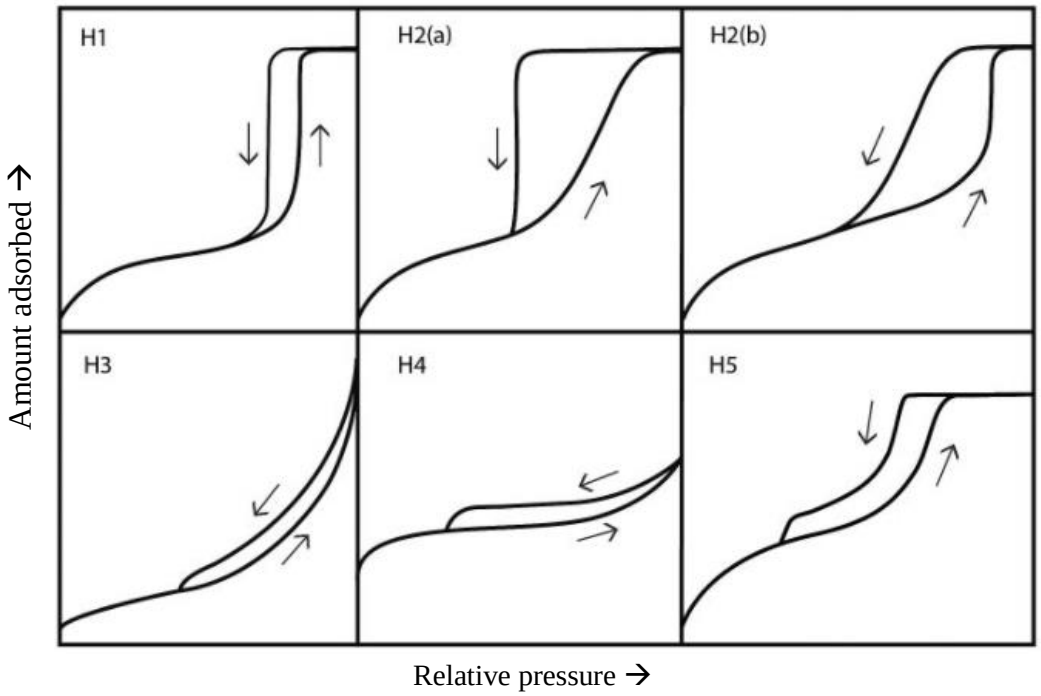

***Figure 16**. IUPAC classification of the hysteresis types*[67].

Experimental procedure

The analysis was carried out in a fully automated Micrometrics TRISTAR II 3020 equipment using N_2 at -196 °C. Each sample was made by weighting about 0.30 g of catalyst and outgassing it at atmospheric pressure and 300 °C for 10 h, in order to remove moisture adsorbed molecules and possible condensates, which may have interfered with the results of the analysis. The adsorption branch was obtained by adding successive volumes of N_2 to the sample and recording the equilibrium pressure, from the lowest up to the saturation one (< $1 \cdot 10^{-3}$ kPa -

≈101.3 kPa). The desorption branch was afterwards obtained by removing known volumes of N_2 and registering values of equilibrium pressure until the reaching of the closed hysteresis.

The specific surface area was calculated using the method proposed by Brunauer, Emmet and Teller (BET), equation *3.6*, in the relative pressure range 0.05 – 0.35:

$$S_{BET} = \frac{V_m \cdot N_A}{V_{mol}} \cdot A_m \qquad (3.6)$$

where V_m is the adsorbate volume of monolayer, V_{mol} is the molar volume of adsorbate (34.65 cm^3/mol for N_2), A_m is the adsorbate cross sectional area (16.2 $Å^2$ for N_2) and N_A is Avogadro's number.

The pore size distribution was determined according to the Barret-Joyner-Halenda (BJH) method, equation *3.7*, considering the entire desorption branch in the partial pressure range from 0.99 to 0.40:

$$d_P = \frac{4 \cdot \sigma \cdot V_{ads} \cdot cos\theta}{RT \cdot \ln\left(\frac{P}{P_0}\right)} + 2t_l \qquad (3.7)$$

In this equation, d_p is the pore diameter, σ is the surface tension of the adsorbate (8.9 mN/m for N_2), θ is the contact angle between condensed phase and the solid walls, R is the gas constant, T is the temperature and t_l is the adsorbed layer depth.

3.3.6 Hydrogen chemisorption

Chemisorption is the most common method used for measuring the metallic dispersion of a sample, a parameter that describes the relation between the number of surface metallic atoms N_s and the total number of metallic atoms N_{tot}. A typical gas used for this type of analysis is H_2, thanks to its weak affinity with the support and the good physisorption on the metal surface, and the ways in which H_2 can be added are several. In the specific case hydrogen, at progressively higher pressures, is added to the sample to be selectively adsorbed at constant temperature. But not only chemisorption can happen, as non-selective adsorption (physisorption) can also occur under certain conditions, and, for this reason, the isotherms obtained are a sum of chemisorption and physisorption. In order to obtain only the chemisorbed quantity, the hydrogen adding is followed by vacuum, which is able to remove the amount of physiosorbed hydrogen from the sample. A new isotherm is this way obtained, which is simply the difference between the former and the latter.

Experimental procedure

To obtain the information on the Ni dispersion, the equipment Micrometrics ASAP 2020C, equipped with a Chemisorption Controller, was used not only for the analysis, but also for the pre-treatment. About 0.30 g of catalyst, reduced at 700 ºC and passivated, were weighted for each sample and then degasified under vacuum at 110 °C for the first 30 min, at 350 °C for the next 60 min, and finally at 100 °C for 30 min in order to help the detachment of undesired molecules. Then, the sample was reduced in hydrogen flow at 350 °C for 1 h (temperature and time long enough to reduce the passivated layer), and then again a degasification phase under vacuum was carried out at 360 °C for 90 min and at 110 °C for 1 h, in order to eliminate the physiosorbed hydrogen. Subsequently the sample was cooled down to 35 °C and a final evacuation and feeding of H_2 were done to obtain the chemisorption isotherm.

To obtain the metallic dispersion values, it is necessary to calculate the number of superficial metallic atoms of the catalyst by using the following equation (*3.8*):

$$N_s = \frac{V_m \cdot N_A \cdot X}{V_{mol}} \qquad (3.8)$$

where X is the number of adsorbed gas atoms per accessible metallic atom, N_A is the Avogadro's number, V_m is the volume of adsorbed gas for the monolayer (mL/g) and V_{mol} is the molar volume of the gas (mL/mol).

After the evacuation, it is possible to determine the metallic dispersion and, starting from there, the total number of metallic atoms using the equation (*3.9*):

$$D_{Ni}(\%) = \frac{N_S}{\frac{G N_A}{M_m}} = \frac{N_s}{N_{TOT} \cdot f_{Ni,red}} \times 100 \qquad (3.9)$$

where G is the metallic content of the catalyst (g_{metal}/g), M_m is the molecular weight of the metal, N_{TOT} is the number of atoms per gram of catalyst, and $f_{Ni,red}$ is the fraction of the nickel reduced at 700 °C.

3.4 REACTION SYSTEM

In this section, the reaction system and the operating conditions in which the glycerol HDO was conducted are described. All the equipment mentioned are available in the laboratories of the research group "Chemical Technologies for Environmental Sustainability" (TQSA), at the Department of Chemical Engineering, Faculty of Science and Technology from UPV/EHU.

3.4.1 Reaction equipment

The catalytic activity measurements for the glycerol HDO were performed in a bench-scale fixed-bed up-flow tubular reactor. The reaction system model is a Microactivity Effi, PID Eng & Tech, controlled by Process@ software. The tubular reactor made in AISI 316 stainless steel, with an internal diameter of 4.6 mm, a height of 305 mm and a stainless-steel frit, is normally placed into a furnace. The temperature of the catalyst bed, inside the reactor, is controlled by a K-type thermocouple inserted through the upper part of the reactor. A PID controller receives the signal measured by the thermocouple and sends another signal to regulate the resistance, which provides the necessary heat to reach the desired temperature.

The system is also provided with a gas feed section and a liquid feed section. The gas inlet lines (H_2, O_2 and He) have a cut-off valve and an EL Flow flowmeter (Bronkhorst High-Tech) for the flow regulation. For pumping the liquid two piston pumps were available: a GILSON 307 (able to pump flows from 0.002 to 5 cm^3/min) and an Eldex 5985 optos 1LMP (for flow rates between 0.002 to 2.5 cm^3/min). The system has the possibility to bypass the He flow at the output of the reactor or to continue along with the other gases thanks to a 6-way valve, that allows the introduction of gases and liquid in the reactor.

Gas and liquid lines are mixed and pre-heated inside the hot box zone at 100 °C with the aim of avoiding a potential condensation in the lines and the elements of the system. The process diagram of the experimental setup is shown in ***Figure 17***.

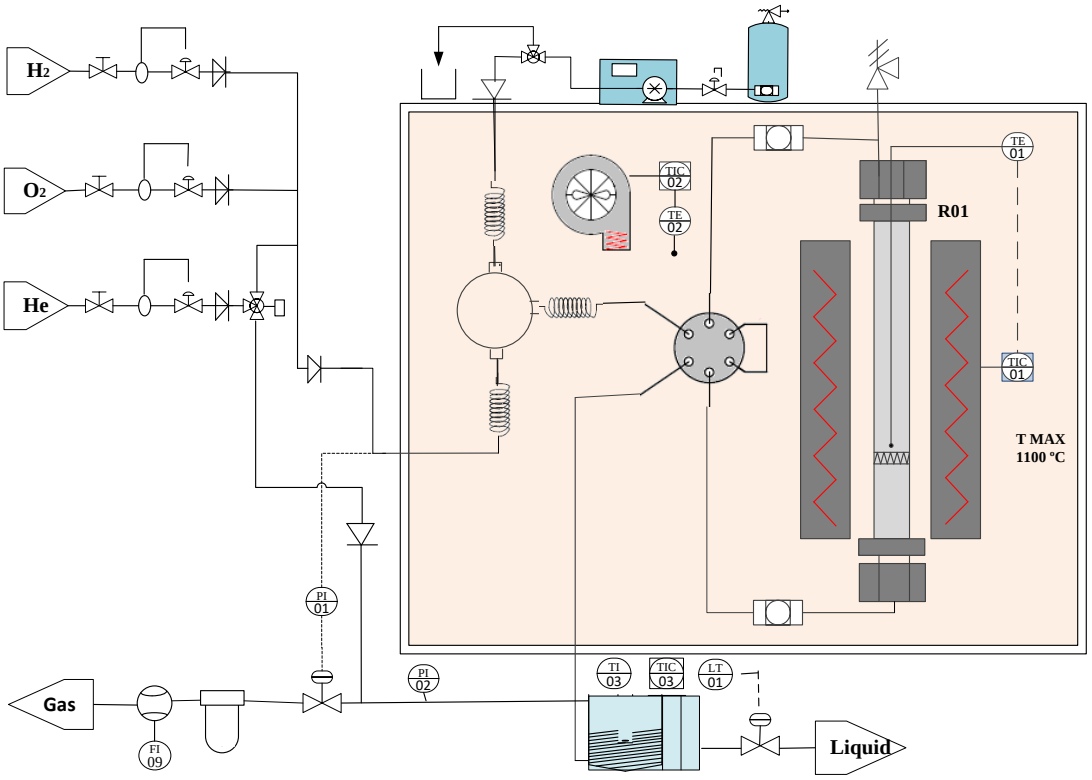

***Figure 17**. Diagram of the experimental setup*

3.4.2 Operating conditions

The evaluation of the catalysts performance has been achieved by carrying out the reaction, for each catalyst, under the same conditions of pressure, temperature, and liquid flow. The values of these parameters have been taken from literature as the best for HDO.

Once the results were obtained and compared, for the catalysts that showed the best performance, it has been decided to carry out additional reactions by maintaining the previous values of pressure and temperature but changing the value of the liquid flow (which was doubled), in order to evaluate the effect of WHSV on the reaction performance.

In a typical catalytic test, 0.5 g of catalyst, with particles size between 0.04 – 0.16 mesh, were placed on the stainless-steel frit and covered with a quartz wool plug. Before carrying out the reaction, the catalyst was reduced *in-situ* under 10%H_2-He flow (50 cm^3/min) at 700 °C, for 60 min, at atmospheric pressure. Subsequently, thanks to the He flow (40 cm^3/min), pressure was increased to the desired value (45 bar). Once the value was reached, the He flow was switched to bypass and a 10 wt.% glycerol aqueous solution was pumped into the reactor with a flow of 0.1 mL/min, while the temperature was raised at 5 °C/min to the desired reaction temperature

(235 °C). The reactor exhaust stream, which consisted of a G-L mixed phase, was cooled down by Peltier cell and the two phases were subsequently separated and analysed: the gas products by microGC and the liquid products by GC-FID and TOC. The HDO performance of catalysts was compared operating at WHSV = 1.2 g_{cat}/g_{gly}, while for studying the effect of this parameter, it was increased to 2.4 g_{cat}/g_{gly}.

3.5 REACTION PRODUCTS ANALYSIS

This section describes the techniques and the procedures used to analyse the liquids products of the reaction.

3.5.1 Gas chromatography (GC-FID)

Gas Chromatography (GC) is a technique able to separate different components of a mixture. This separation depends on the different interaction strength of the molecules with a mobile phase and a stationary phase within the GC column. The mobile phase, that is generally an inert gas, carries the mixture through the column. The molecules are then repeatedly absorbed and desorbed by the stationary phase and, depending on the affinity of the molecules with the stationary phase, they are slowed down and they show, therefore, different retention times for different given analysis conditions. Thus, components with different affinities for the stationary phase (different retention times) are physically separated, detected and analysed. Many different types of detectors exist and, among all of them, the Flame Ionization Detector (FID) has been used, which is characterised by good sensitivity, ample range of linearity and excellent stability. This detector typically uses H_2/Air flame to oxidise organic molecules and, when the sample passes through it, electrically charged particles are formed. The ions are so collected and an electrical signal is finally produced and measured. This technique has been used to analyse the liquid products.

Experimental procedure

The samples of the liquid product were collected at desired times (every hour starting from the first) in 2 mL vials and were kept refrigerated until the analysis was conducted.

The operating conditions employed are specified in the ***Table 2***:

***Table 2**. GC-FID analysis conditions.*

Chromatograph	Agilent 6890N
Temperature (°C)	300
Flow (cm^3/min)	H_2: 40.0 Air:350.0 Combined flow: 17.0
Carrier gas	Makeup gas: N_2 H_2
Columns	HP-Wax Bonded Polyethylene Glycol (25.0 m x 200 μm x 0.40 μm)
Column flow (cm^3/min)	1.0
Oven	80 °C for 4 min, up to 110 °C during 15 min and, finally, 200°C for 10 min. Ramp of 30 °C/min
Loop / Injection volume	3 μ
Injector	Split 20:1
Analysis time	33 min
Control system	GC ChemStation

3.5.2 Total organic carbon (TOC)

During the reaction, many water-soluble intermediates are produced and are quite difficult to detect or identify by chromatographic analysis. In order to estimate the total amount of organic products in the samples, TOC analysis was used. The obtained parameter is a measure of the total mass of carbon, which represents the various organic compounds present in the water solution. It was then possible to calculate the carbon conversion to gas X_{gas}.

TOC analysis is based on a combustion/non-dispersive infrared gas method. The samples are completely oxidized by heating up to 680 °C in an oxygen-rich environment, created into combustion-tubes filled with a platinum catalyst. Depending on the bonding condition and the type of atoms constituting each molecule, infrared radiation of different wavelengths are absorbed and carbon dioxide is generated, and the amount of rays finally absorbed is proportional to the gas density. The amount of absorbed rays is measured by an infrared gas analyser (NDIR), and it is so possible to trace the gas density's value. NDIR is also able to

detect inorganic carbon (IC) through the sparging process, while the total carbon (TC) concentration is calculated thanks to a standard calibration curve. Thus, TOC concentration can be simply calculated by subtracting the IC from the TC concentration, but, since the IC values were negligible, Carbon conversion to gas has been directly calculated from the TC.

Experimental procedure

The TC value was measured off-line on a Shimadzu TOC-L series apparatus equipped with an autosampler. Before analysis, 350 µL of liquid samples were diluted in 50 mL of ultrapure water (Milli-Q) to reach the standard range between 100 and 1000 mg_{carbon}/L. Each analysis was repeated 3 times.

3.6 DEFIFINITIONS AND CALCULATIONS

In this work, *Weight Hourly Space Velocity* (WHSV, g_{cat}/g_{gly}) was calculated as the ratio of the feed mass flow and the catalyst's mass:

$$WHSV\ (g_{cat}/g_{gly}) = \frac{\dot{m}_{feed}}{m_{cat}} \qquad (3.10)$$

The *Conversion of glycerol* (X_{Gly}) was calculated starting from GC-FID data, using the obtained values of glycerol concentration present in the feeding and in the samples at the desired time:

$$X_{gly}\ (\%) = \frac{C_{gly}^{in} - C_{gly}^{out}}{C_{gly}^{in}} \times 100 \qquad (3.11)$$

The *Carbon conversion to gas* (X_{gas}) was calculated on the basis of carbon molar flow as follows, using data obtained by TOC analysis:

$$X_{gas}\ (\%) = \frac{F_C^{in} - F_C^{out}}{F_C^{in}} \times 100 \qquad (3.12)$$

The *Carbon conversion to liquid* (X_{liq}) was calculated as the total carbon left in the liquid outlet multiplied by the glycerol conversion:

$$X_{liq}\ (\%) = (100 - X_{gas}) \cdot X_{gly} \qquad (3.13)$$

The *Degree of deoxygenation* (DDO) of glycerol was calculated as the fraction of the oxygen atoms present in the flow out per oxygen atoms present in the feeding flow:

$$DDO\ (\%) = \frac{F_{products}^{out}}{F_{gly}^{in}} \times \frac{x}{3} \times 100 \qquad (3.14)$$

Carbon Selectivity of the liquid products was defined as the fraction of the carbon atoms converted per converted glycerol:

$$CS_i\ (\%) = \frac{C_x^{in} - C_x^{out}}{C_{gly}^{in} - C_{gly}^{out}} \times \frac{x}{3} \times 100 \qquad (3.15)$$

Efficiency in hydroxyacetone (HA), propylene glycol (PG) and ethylene glycol (EG), which are the major products of the reaction, was calculated as the ratio of the mass of fed glycerol and the mass of obtained product:

$$\eta_i = \frac{m_i}{m_{gly}} \qquad (3.16)$$

4. RESULTS AND DISCUSSION

In this chapter, the experimental results are presented and discussed. First, in section 4.1 the characterization of the catalysts, both in their calcined and reduced forms, is treated; afterwards, in section 4.2, the results of catalytic activity studies are reported and discussed, in order to find the correlation between the observed physicochemical properties and the catalytic performance.

4.1 CATALYSTS CHARACTERIZATION

4.1.1 Bulk chemical composition and textural properties

For the x-WNiAl solids synthesised by sol-gel, the nominal tungsten loadings were 1, 3, 5, and 9 wt. %. A TGA experiment was carried out in advance to measure the hydration degree of the precursor salt of W. The weight loss and its derivative in function of temperature are shown in ***Figure 18.***

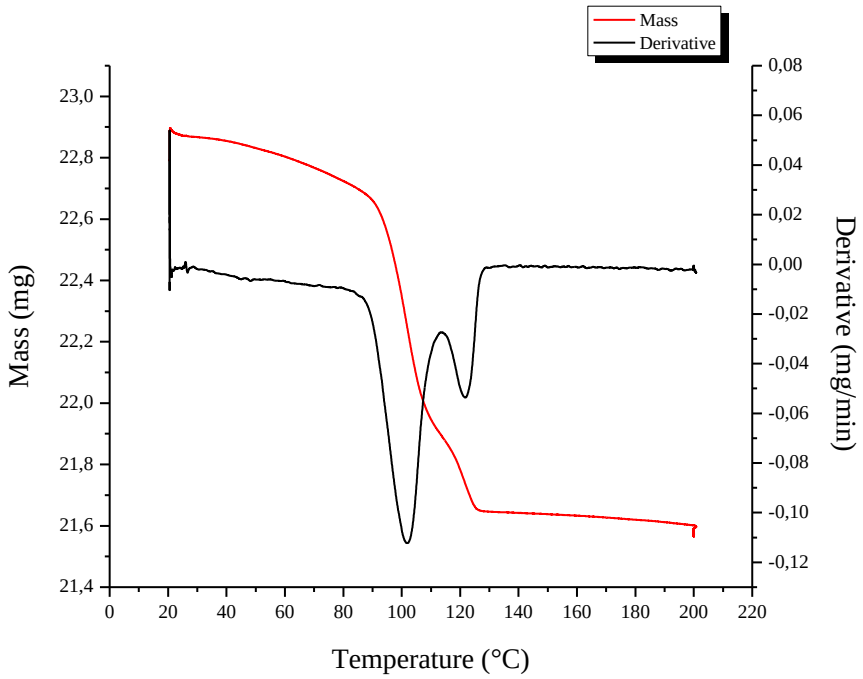

Figure 18*. TGA analysis of W precursor salt.*

The W precursor salt showed two main weight loss events: one at lower temperature, from 85 to 115 °C with a maximum at 102 °C, ascribed to the loss of hydration water; another at higher temperature, with a maximum at 122 °C, related to the loss of nitrates. According to the obtained results, the hydration degree estimated was 2.5 wt. %.

To check the effective content in doping agent, besides the ratio Ni/Al, the bulk molar composition was evaluated by XRF analysis, and the results are shown in ***Table 3***:

Table 3*. Chemical composition of the catalysts obtained by XRF.*

Catalyst		***Metallic content***		
	Ni/Al	**Ni (% wt)**	**Al (% wt)**	**W (% wt)**
0-WNiAl	0.52	34.4	30.4	0.0
1-WNiAl	0.49	31.3	29.2	0.8
3-WNiAl	0.49	30.3	28.5	2.2
5-WNiAl	0.50	29.8	27.2	4.1
9-WNiAl	0.49	28.0	26.3	7.1
1W/NiAl	0.50	30.3	27.6	0.8

The tungsten contents resulted to be systematically lower than expected (on average, 21% lower for the solids prepared by sol-gel): since the water content of the precursor salt was taken into account while doing the calculations for the synthesis, these results can only be explained by possible interactions during the XRF analysis between tungsten, nickel and aluminium, which resulted in smaller values of W loadings. Despite this, increasing the amount in weight of doping agent, coherently, the content of Ni and Al decreased, while the molar ratio Ni/Al remained about 0.5 (desired stoichiometric one).

The textural composition, in terms of BET surface area, pore volume and pore size, was investigated both on the calcined catalyst precursors and on the *ex-situ* reduced ones, via nitrogen physisorption. Isotherms of adsorption and distribution of the pore size profiles were obtained through this analysis.

In general, comparing the obtained isotherms of adsorption with the standard ones, it is possible to notice that the synthetised catalysts gave Type IV isotherms, characteristic for mesoporous solids. The adsorption behaviour in mesopores is determined by the adsorbent-adsorptive interactions and by the interactions between the molecules in the condensed state. The initial monolayer-multilayer adsorption of N_2 on the mesopore walls, which takes the same path as the corresponding part of a Type II isotherm, is followed by pore condensation. The phenomenon of pore condensation consists in the gas transition to a liquid-like phase, in a pore, at a specific pressure P lower than the saturation pressure P^0 of the bulk liquid[70,69]. A typical feature of Type IV isotherms is the final saturation plateau, of variable length and sometimes reduced to only an inflexion point. In particular, Type IV(a) isotherms were obtained, where capillary condensation is accompanied by hysteresis, specifically, H1 type hysteresis. Type H1 loop is generally found in materials which exhibit a narrow range of uniform mesopores.

Usually, network effects are minimal, while the steep and narrow loop is a sign of delayed condensation on the adsorption branch[71].

In ***Figure 19*** and ***Figure 20*** the results given by the calcined and reduced catalysts with different amounts of tungsten are compared.

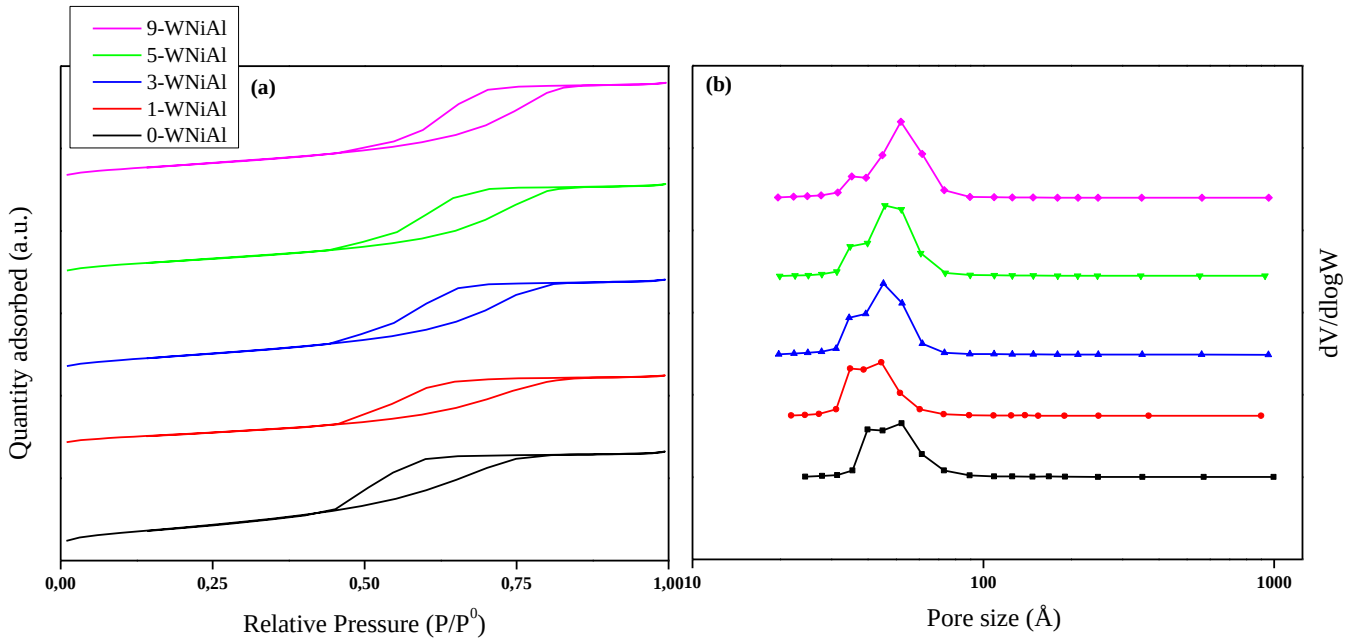

Figure 19. *Comparison of the results given by the calcined catalysts with different W-loadings:* ***a)*** *Isotherms of adsorption/desorption;* ***b)*** *Change in pore distribution.*

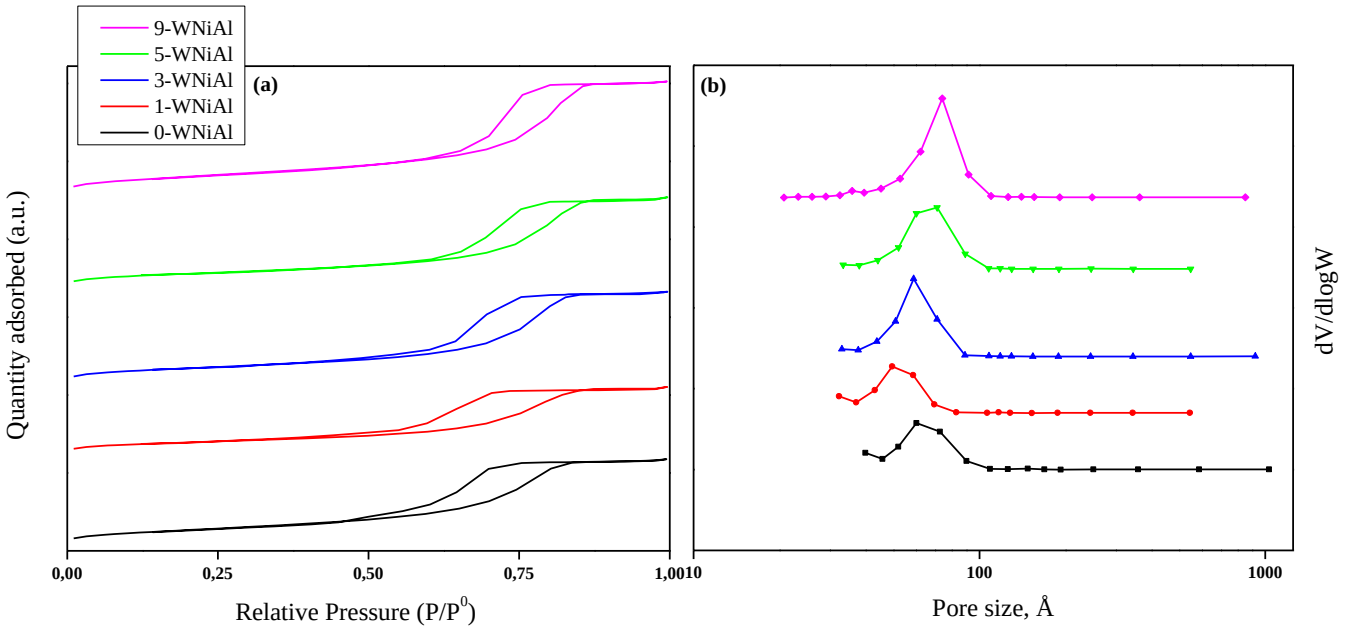

Figure 20*. Comparison of the results given by the reduced catalysts with different W-loadings:* ***a)*** *Isotherms of adsorption/desorption;* ***b)*** *Change in pore distribution.*

Among the sol-gel synthesised solids, the isotherms of adsorption/desorption did not present big differences in their shape, neither when the amount of doping agent added was different nor when the catalyst was calcined or reduced. Looking at the pore size distribution, instead, it is possible to notice that there was not an evident change between the calcined and the reduced samples, but, looking at the differences between the results given by the various W loadings, the change is evident. The bigger the amount of doping agent added, the more the pore size distribution was shifted to bigger values: the peak for the catalyst 1-WNiAl was at about 50 Å, while the peak for 9-WNiAl was around 75 Å.

In ***Figure 21*** and ***Figure 22*** the comparison is made between the two calcined and reduced catalysts, respectively, prepared with the same amount of dopant (1 wt. %) but via different synthesis method. Again, the isotherms of adsorption did not change visibly: they maintained the same shape after reduction and among the two different preparation methods. Comparing the pore size distribution, it can be observed that it was similar between the two differently synthesised solids, the peak was close to 50 Å for both the sol-gel and the impregnated. Analysing the differences between the calcined and the reduced samples, the 1W/NiAl catalyst presented a small shift of the peak to a bigger pore size, while the 1-WNiAl did not. Thus, the sol-gel synthesised catalyst presented a bigger resistance to pore size distribution changes after reduction.

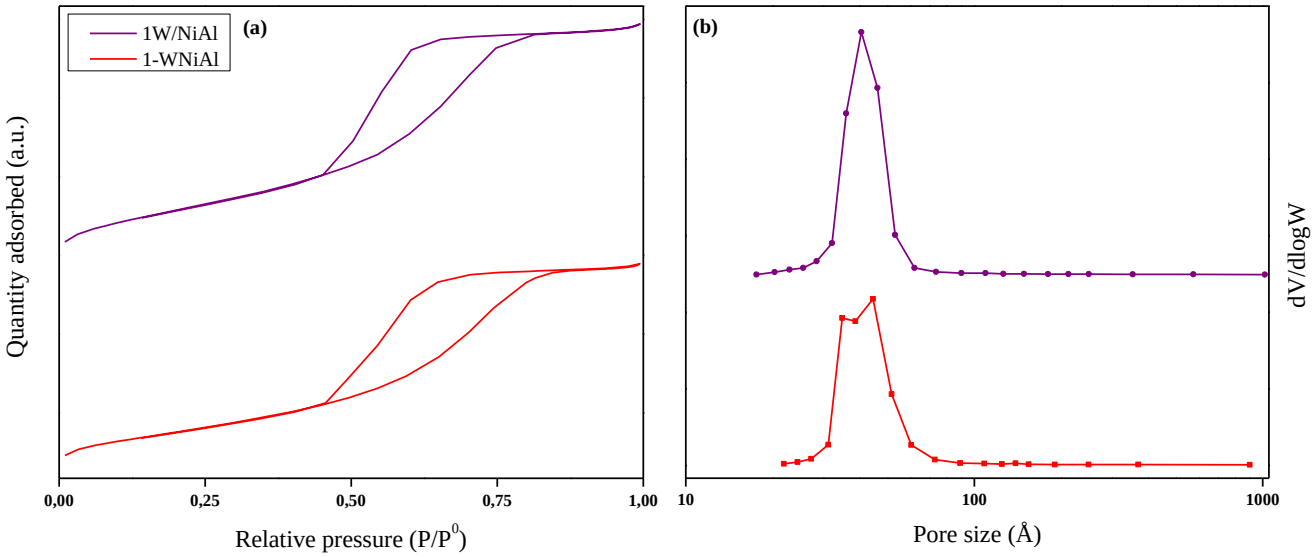

Figure 21. *Comparison of the results given by the calcined catalysts prepared with different synthesis methods:* ***a)*** *Isotherms of adsorption/desorption;* ***b)*** *Change in pore distribution.*

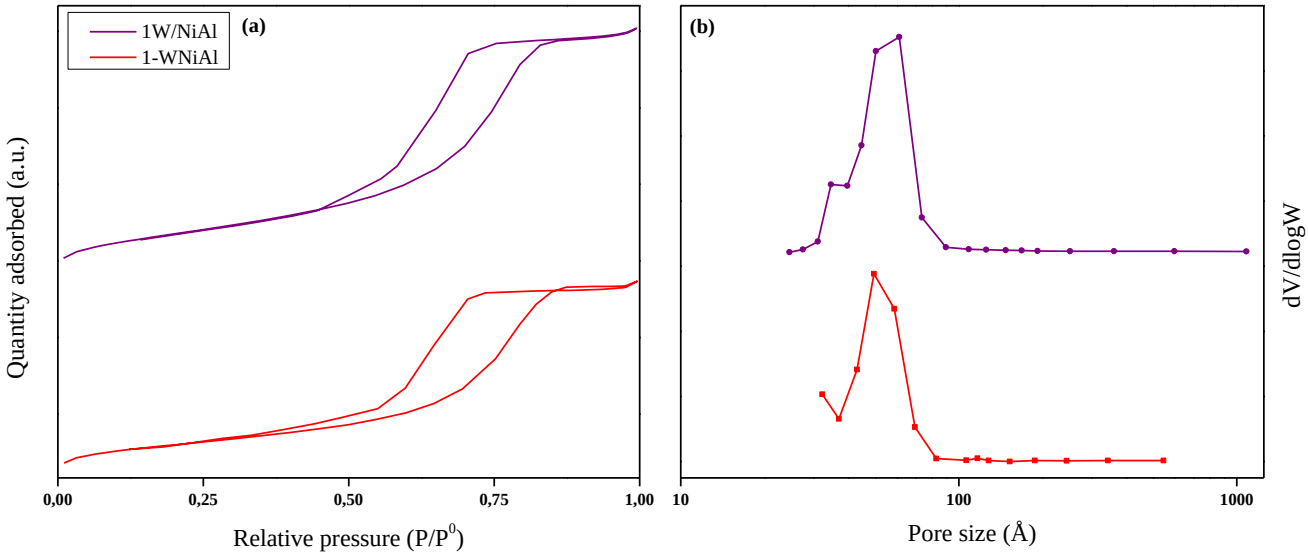

***Figure 22**. Comparison of the results given by the reduced catalysts prepared with different synthesis methods: **a)** Isotherms of adsorption/desorption; **b)** Change in pore distribution.*

The results of the analysis are shown in the ***Table 4***:

***Table 4**. Results of the nitrogen physisorption analysis in terms of BET surface, pore volume and pore size.*

	Catalyst	**S_{BET} (m^2/g)**	**V_P (cm^3/g)**	**D_P (Å)**
Calcined	*0-WNiAl*	65	0.089	56
	1-WNiAl	41	0.066	65
	3-WNiAl	55	0.086	63
	5-WNiAl	53	0.086	65
	9-WNiAl	51	0.090	71
	1W/NiAl	55	0.077	56
Reduced	*0-WNiAl*	43	0.082	74
	1-WNiAl	32	0.062	77
	3-WNiAl	43	0.087	80
	5-WNiAl	41	0.085	82
	9-WNiAl	52	0.110	81
	1W/NiAl	42	0.078	74

Observing the obtained data of S_{BET} for the calcined samples with different amounts of tungsten, a maximum value was given by the sample loaded with 3 wt. %, to then decrease for higher dopant loadings. The same phenomenon is not observable in case of reduced samples, where the largest value of S_{BET} was shown by 9-WNiAl. Indeed, comparing the data before and after reduction, it was found that there was a decrease of about 22% in the S_{BET} values of all the reduced catalysts, but not for the 9 wt. % loaded, which did not show any decrease.

Comparing the two catalysts prepared via different synthesis methods, the measured specific surface area for the impregnated one resulted to be bigger than the counterposed sol-gel one, both in case of calcined and reduced samples (in the first case it was 34% bigger, in the second 31%). It is interesting to notice that the decrease in S_{BET} value after reduction was of 23%, similar to the results obtained for the sol-gel catalysts.

To conclude, the increase in the amount of doping agent went together with a slight increase of the values of pore volume and pore size, probably because of the bigger size of tungsten itself and its presence in the structure of the systems.

4.1.3 Nature and morphology of the phases

To identify the featured phases in both the catalysts precursors and the *ex-situ* reduced ones, the powder XRD analysis was carried out. The obtained diffractograms are reported in ***Figure 23***.

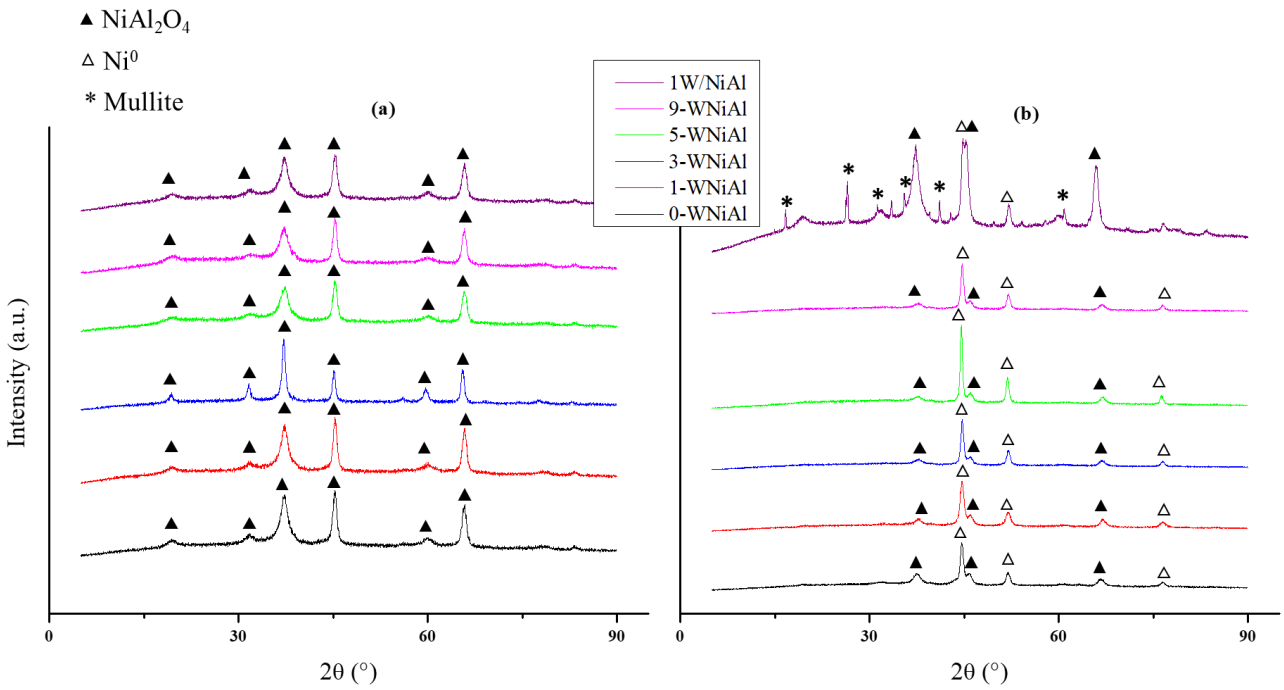

***Figure 23**. XRD patterns **a)** before reduction **b)** after reduction.*

The diffractogram related to reduced 1W/NiAl is not properly clear: some quartz wool (mullite) was in the sample because of the *ex-situ* reduction process, and its signals (ICDD-PDF 98-008-0384) appeared during the analysis. Anyway, there were not overlaps between the diffraction lines, so, it was possible to identify and integrate the peaks connected to the investigated species.

Looking at the diffractograms related to the calcined solids, the most prominent features of XRD patterns are ascribed to cubic spinel structure (ICDD-PDF 78-0552): the diffraction lines at 2θ = 37.010 °, 44.997 °, 59.663 ° and 65.537 ° confirmed the formation of the spinel. No other signals of other possible phases (like NiO, inverse spinel or WO_x) were present: this means that practically all the synthesised solids formed the desired structure. When observing the XRD patterns of the solids after reduction at 700 °C, diffraction lines of the spinel lose intensity, while characteristic features of metallic nickel (ICDD-PDF 00-004-0850) are evident (2θ = 44.497 °, 51.851 ° and 76.383 °): sign of the fact that Ni^0 clusters were formed. No other peaks from W or γ-Al_2O_3 (which should be present in the solid) were detected on reduced samples.

From the peaks integration and the use of Scherrer's equation, crystallite sizes and structural parameters were calculated and reported in ***Table 6***. To obtain the $NiAl_2O_4$ crystallite size the peaks at 37.010 °, 44.997 ° and 65.537 ° were considered, while for Ni^0 at 51.851 ° and 76.383 °.

Table 6. Structural parameters obtained through XRD analysis.

	Catalyst	$\tau_{NiAl2O4}$ **(nm)**	τ_{Ni^0} **(nm)**	**a (Å)**
Calcined	*0-WNiAl*	10.3	-	8.031
	1-WNiAl	12.1	-	8.018
	3-WNiAl	10.9	-	8.032
	5-WNiAl	10.8	-	8.018
	9-WNiAl	12.1	-	8.025
	1W/NiAl	10.8	-	8.021
Reduced	*0-WNiAl*	8.2	13.5	7.942
	1-WNiAl	9.1	10.6	7.904
	3-WNiAl	7.7	14.9	7.916
	5-WNiAl	9.4	18.1	7.921
	9-WNiAl	8.6	17.2	7.920
	1W/NiAl	9.3	15.6	8.013

From the data it can be noticed that the experimentally measured lattice parameter for unreduced samples remained quite stable at values very close to the one of stoichiometric nickel aluminate spinel (8.0451 Å)[72]. When the precursors were reduced, a lattice compression could be highlighted and explained by the migration of the Ni^{2+} ions forming the nickel aluminate lattice to the surface, suggesting, moreover, a simultaneous enrichment of the bulk in alumina. The changes in lattice parameter for x-WNiAl, before and after reduction, are shown in ***Figure 24,*** where the compression after reduction is evident. It is also notable that the lattice parameter of reduced x-WNiAl increased with the increase of tungsten loadings, reaching a plateau with

5-WNiAl, that showed almost the same value as 9-WNiAl. This result can be explained by a major quantity of big sized tungsten remaining in the lattice when Ni^{2+} in the spinel structure was reduced to Ni^{0} and migrated to the solids surface.

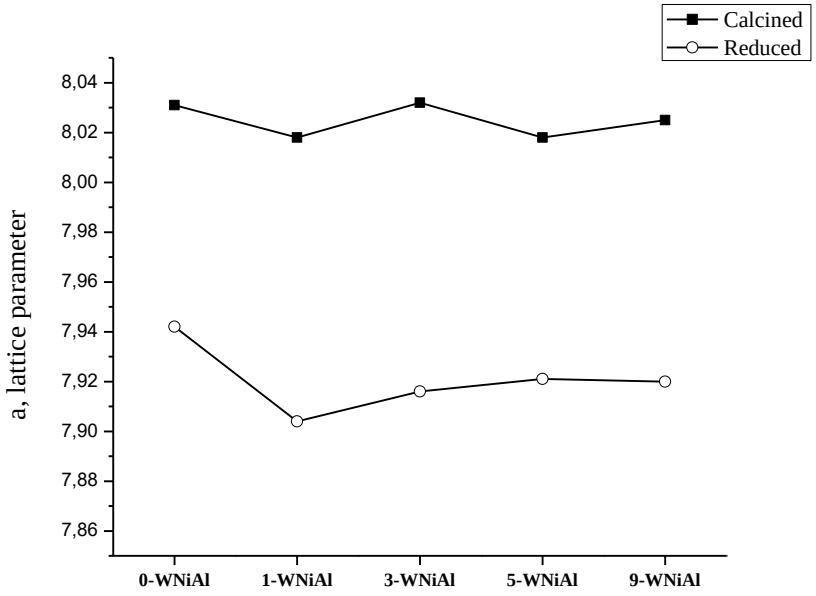

***Figure 24**. Correlation between W contents and lattice parameter.*

The hypothesis of nickel migration and bulk enrichment in alumina was confirmed by two results. First, by the small shift in 2θ position for the Miller plane (440) from 65.5 ° to 67 °, which is shown in ***Figure 25***. The shift was evident for all the reduced samples, while the trends of 2θ position in function of W loadings remained basically the same, not showing any correlation between the amount of doping agent added and the position of the peak in the diffractogram.

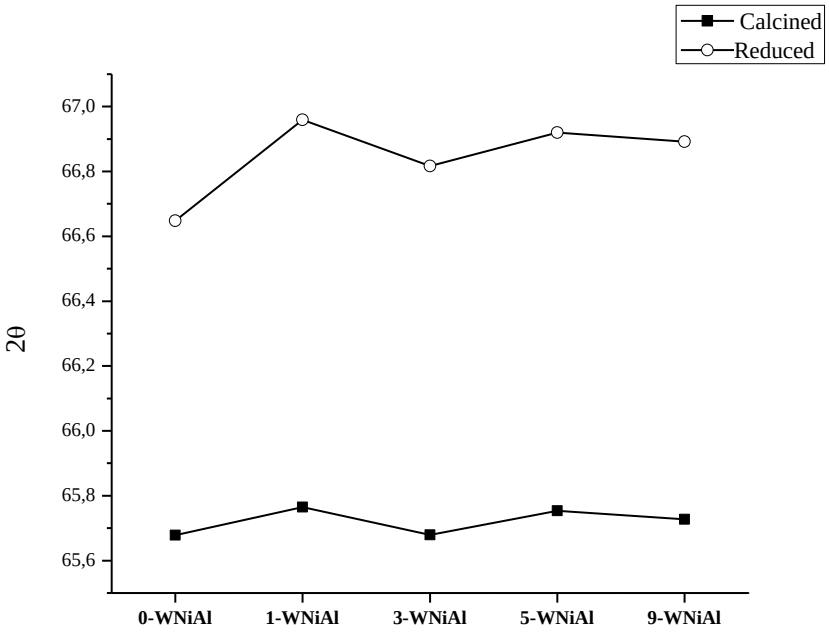

***Figure 25**. Correlation between W contents and 2θ position.*

Second, by the formation of metallic nickel, crystallized into *fcc* structure (***Figure 26***)[5], as can be observed in the diffractograms of all the reduced samples[73]. The relatively small size of the metallic nanoclusters formed in the systems reflected the strong interaction of the nickel with the Ni-Al-O support, which stabilizes Ni nanoparticles and reduces their surface mobility[74]. Crystallite size of nickel aluminate and metallic nickel varied in the 10.8-12.1 nm and 18.1-10.6 nm range, respectively. In both cases, no clear trend in crystal growth was observed with the tungsten loadings, but the bigger dimensions of the Ni^0 crystallites formed in the doped catalysts confirmed the weakening of the Ni-Al interaction.

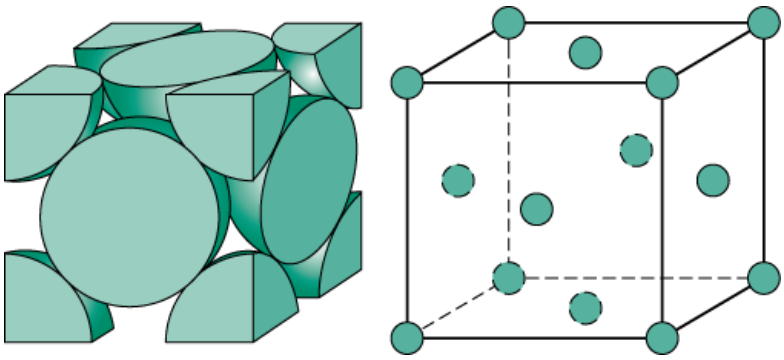

***Figure 26**. Fcc structure of crystallized Nickel after reduction.*

4.1.2 Reducibility of the solids

The reducibility of the samples was studied by temperature programmed reduction analysis (H_2-TPR), and the obtained reduction profiles are shown in ***Figure 27***.

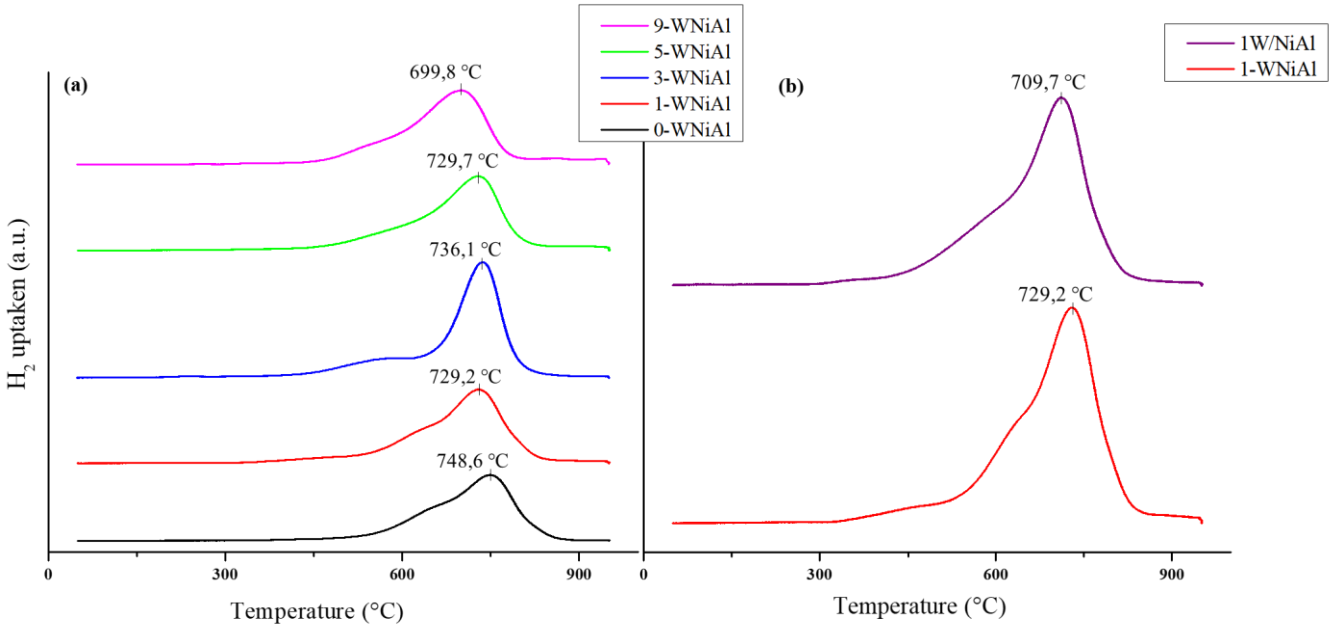

Figure 27*. Reduction profiles for* ***a)*** *catalysts with different amounts of W* ***b)*** *catalysts synthesised via different preparation methods.*

The temperature ramp was decided according to literature; above 600 °C, the Ni^{2+} incorporated in a spinel structure begins to reduce itself[75,76]. In the light of this, the analysis was conducted reaching 950 °C to achieve the reduction of all the nickel. Looking at the TPR profiles, besides the main peaks, left tails are observable in all the curves, which suggest the presence of different species with different reducibility. Studies of reducibility on WO_x, γ-Al_2O_3 doped with 9 wt. % of W and $NiAl_2O_4$ were conducted, and the obtained reduction profiles are reported in ***Figure 28***. WO_x species, obtained by calcination of ammonium metatungstate hydrate up to 850 °C, in agreement with literature, showed two reduction peaks at about 768 and 854 °C, which correspond the reduction of amorphous and non-stoichiometric oxides to metallic tungsten, that occurs in two steps and where the total reaction can be written as: $WO_x + H_2 \rightarrow W^0 + H_2O$[77]. Doped alumina, synthesised via citric acid sol-gel method (using the same salts as for the catalyst precursors) and calcined up to 850 °C, showed H_2 consumption starting from 760 °C. From previous studies conducted by the TQSA research group, it was known that bare γ-Al_2O_3 is not subjected to any reduction under this temperature range, so, the result obtained on doped

alumina, demonstrated that the responsible for the little peak which started at 760 °C are the WOx species present in the structure.

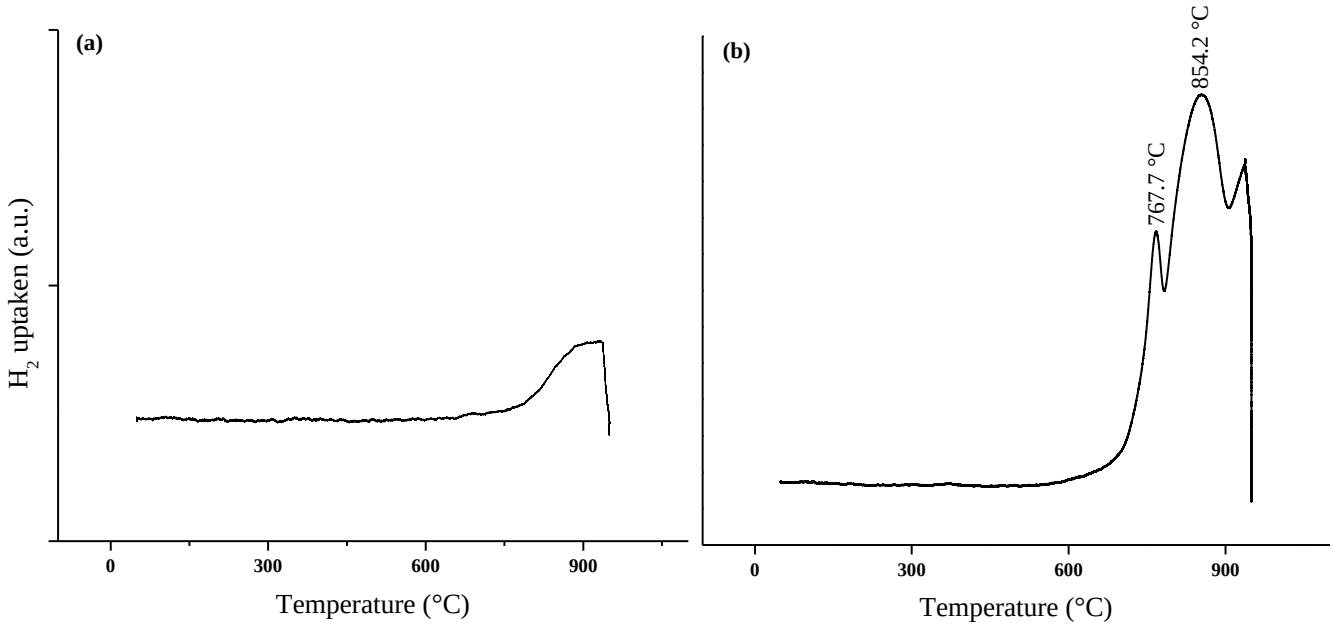

***Figure 28**. Reduction TPR profiles of **a)** doped Al_2O_3 **b)** WO_x.*

Bare $NiAl_2O_4$ (0-WNiAl) showed a TPR curve which can be split into three peaks (low, medium and high temperature): the low temperature peak ascribed to the reduction of easily reducible free NiO[78], formed in weak interaction with the non-stoichiometric nickel aluminates spinel[79]; the medium temperature peak assigned to the reduction of Ni^{2+} species in a defective $Ni_{1-x}Al_2O_{4-x}$ phase; the high temperature peak related to the reduction of Ni^{2+} species in the $NiAl_2O_4$ spinel lattice. Thus, the presence of these species was highlighted by the TPR profiles, but the small dimensions of the tails suggested a lack of free nickel oxide and a main presence of Ni^{2+} species in spinel-like structure, which favours the dispersion of metallic nickel phase formed upon reduction. A proof of this was the small average crystallite size of Ni^0 particles obtained (measured by XRD), since the reduction of NiO species produces large Ni^0 particles[80].

Looking at the position of the main peak in case of the catalysts with different amounts of tungsten (***Figure 27 (a)***), a promotion in the reduction of nickel due to the presence of tungsten was highlighted: indeed, the reduction temperature was progressively downshifted by the tungsten addition, from 748.6 °C for 0-WNiAl to 699.8 °C for 9-WNiAl. Besides, looking at the left tails, it can be noticed that the medium temperature peaks were shifted to lower temperature too. In the light of this, it can be deduced that the W-doping makes the reduction

of nickel easier. Probably some of the W^{x+} ions replaced the Al^{3+} ions surrounding the Ni^{2+} in the spinel structure, resulting in a weakening of the interaction strength between Ni and Al (quite strong in the $NiAl_2O_4$ structure) and in a lowering of the reduction temperatures.

In case of the catalysts prepared with the two different synthesis methods (***Figure 27 (b)***), a downshift to lower temperatures (of about 30 °C) was showed for all the three peaks (low, medium and high) by the catalyst prepared via impregnation. Again, the presence of tungsten, mostly on the catalyst surface, weakened the Ni-Al interactions making easier the reduction of nickel.

From the integration of the peaks, it was possible to calculate the amount of hydrogen consumed by each sample during the temperature programmed reduction, and so, the degree of nickel reduction ($f_{Ni,red}$) . Since for the studies on catalytic activity the synthetised precursors were reduced *in-situ* at 700 °C for 1 h, to have an estimation of the Ni^{2+} effectively reduced under those conditions, the integration was not done over the whole peaks, but from room temperature to 700 °C. Probably, also some W^{x+} ions were reduced under this temperature ramp and, in this case, the values of $f_{Ni,red}$ would have been lower than the calculated ones. The approximation that all the H_2 was consumed to reduce only nickel was done in the light of the obtained reduction profile of WO_x species, which showed the first reduction peak at 768°C. This way, information about the reducibility of the samples were obtained and the values reported in ***Table 5***:

Table 5. *Results of H_2-TPR analysis in terms of H_2 consumption.*

Catalyst	**Total H_2 consumption ($mmol_{H2}/g$)**	**H_2 consumption at 700 °C ($mmol_{H2}/g$)**	**$f_{Ni,red}$** (%)
0-WNiAl	3.80	3.60	61.4
1-WNiAl	5.87	3.66	68.6
3-WNiAl	6.31	4.35	84.1
5-WNiAl	5.48	4.06	80.0
9-WNiAl	6.06	3.86	80.9
1W/NiAl	5.15	3.50	68.2

In agreement with the observations made on the reduction profiles, the fraction of reduced nickel was higher for the catalysts with bigger amounts of tungsten than for the one with 0 and 1 wt. %, confirming that the presence of the dopant facilitates Ni^{2+} reduction. The addition of tungsten, indeed, resulted in higher H_2 consumption values. A proper correlation between the W loadings and the hydrogen consumption values could not be found.

The preparation method did not affect the reducibility of the samples: the fraction of reduced nickel was about 68 % both for 1-WNiAl and 1W/NiAl.

4.1.4 Metallic function

To carry out the HDO of glycerol with *in-situ* produced hydrogen, metallic catalytic sites are required. Once the catalysts precursors were reduced at 700 °C for 1h and the Ni^0 was formed (as confirmed by XRD), it was interesting to measure the final accessible metallic nickel surface and how it was affected by the additions of dopant. To evaluate the Ni dispersion of the samples, and so to describe the relation between the number of surficial nickel atoms and the number of total nickel the static hydrogen chemisorption was used. The analysis was conducted on the *ex-situ* reduced solids and results are all shown in ***Table 7***.

Table 7*. Results of hydrogen chemisorption analysis in terms of H_2 chemisorbed, surface of metallic Ni available per gram of catalyst and Ni dispersion.*

Catalyst	**H_2 Chemisorbed ($mmol_{H2}/g_{cat}$)**	**S_{Ni}^0 (m^2/g_{cat})**	**D_{Ni} (%)**
0-WNiAl	0.018	1.2	1.30
1-WNiAl	0.037	2.9	2.77
3-WNiAl	0.046	3.0	0.48
5-WNiAl	0.025	1.2	0.25
9-WNiAl	0.018	0.9	0.12
1W/NiAl	0.018	1.8	0.44

Thanks to TPR, it was deduced that Ni reduction was easier for doped samples. However, a maximum value of S_{Ni}^0 was shown by the sample 3-WNiAl: this is probably due to the increase of crystallites size (τ_{Ni}), calculated through XRD, observed for the catalysts with a tungsten content higher than 3 wt. %, as highlighted in ***Figure 29***.

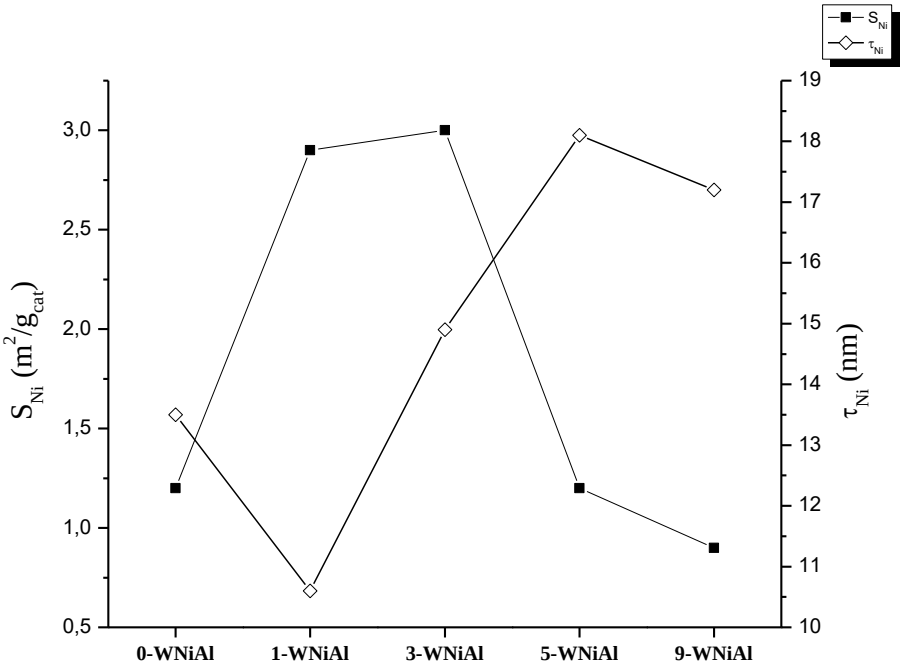

***Figure 29**. Comparison of S_{Ni}^0 and τ_{Ni} trends for the x-WNiAl catalysts.*

Another explanation for the S_{Ni}^0 value given by the sample with 3 wt. % of W, which was quite off the trend, can be the formation of Ni-W alloys that were not detected by XRD.

The obtained dispersion values for the doped solids showed a notable decrease when the amount of tungsten was increased: the changes were probably due simply to the lower amount of Ni present in the catalysts. Anyway, the doping agent was added to the system in order to enhance the acid capacity, and not to have an effect on the metallic dispersion.

Paying attention to the preparation method, instead, and comparing the results given by the two catalysts with 1 wt. % of W loading, a huge difference between the metallic dispersion values is noticeable: the D_{Ni} given by the sol-gel sample was almost 9 times bigger than the one given by the impregnated one. Probably, when the catalyst was prepared via impregnation method, the tungsten covered nickel surface, causing a lower value of nickel dispersion and a consequent lower availability of metallic catalytic sites.

4.1.5 Acid sites on the catalyst surface

The catalytic reactions involved in the HDO of glycerol are strongly influenced by acid-base properties: for this reason, the study of these functionalities was needed for a good interpretation of the activity and selectivity data. As previously explained, the oxophilic doping agent was to increase the acidity of the catalysts and enhance, this way, the dehydration and C-O bonds scission capacity. To evaluate this property, the temperature-programmed desorption of ammonia analysis was used (NH_3-TPD). Ammonia, being a small sized and basic molecule, can be easily adsorbed onto the acid sites of the doped catalysts surface, and then desorbed thanks to a temperature increase[81]. Starting from the amount of ammonia that was adsorbed by each catalyst, it was possible to calculate the values of acidity and its total density, which are reported in ***Table 8***:

Table 8*. Results of NH3-TPD analysis in terms of acidity of the catalyst and density of the total acidity.*

Catalyst	**Acidity ($\mu mol_{NH3}/g_{cat}$)**	**Density of the total acidity ($\mu mol_{NH3}/m^2$)**
0-WNiAl	138.4	3.2
1-WNiAl	143.5	4.5
3-WNiAl	179.2	4.1
5-WNiAl	172.8	4.2
9-WNiAl	218.4	4.2
1W/NiAl	217.9	5.2

As expected, it can be noticed how the acidity increased with the quantities of doping agent added: the higher the amount of tungsten, the higher the acidity. The 9 wt. % loaded sample presented a total acidity 58% higher when compared to the not doped one (218.4 vs 138.4 μmol NH_3/g_{cat}, respectively).

Regarding acid sites density, it seemed to be independent from the W loading, while it was not from the preparation method: the density of total acidity value for 1W/NiAl was 15 % higher than the one for 1-WNiAl. Probably when the impregnation method is used, with more tungsten staying on the surface, a higher availability of the acid sites (confirmed by higher values of acidity and its density) is the consequence.

4.2 CATALYTIC ACTIVITY IN GLYCEROL HDO

The catalytic activity of the synthesised catalysts in glycerol HDO was evaluated in a continuous tubular reactor, at a temperature of 235 °C and a pressure of 45 bar, over *in-situ* reduced x-WNiAl and 1W/NiAl catalysts, with a feeding of an aqueous solution of glycerol 10 wt. %.

In the section, results in terms of glycerol conversion, deoxygenation degree, efficiency and selectivity towards major prodcuts are reported. The samples for catalytic studies were taken and analysed after 3 h of reaction since it was known, from previous studies, that it was the time in which the best results were obtained.

4.2.1 Effect of tungsten content

To evaluate the effect of tungsten content on the catalytic activity of W-doped catalysts synthesised by sol-gel, the selected WHSV was 1.2 g_{cat}/g_{gly}. The obtained conversion of glycerol (X_{gly}), carbon conversion to gas (X_{gas}) and degree of deoxygenation (DDO) are shown in ***Figure 30***.

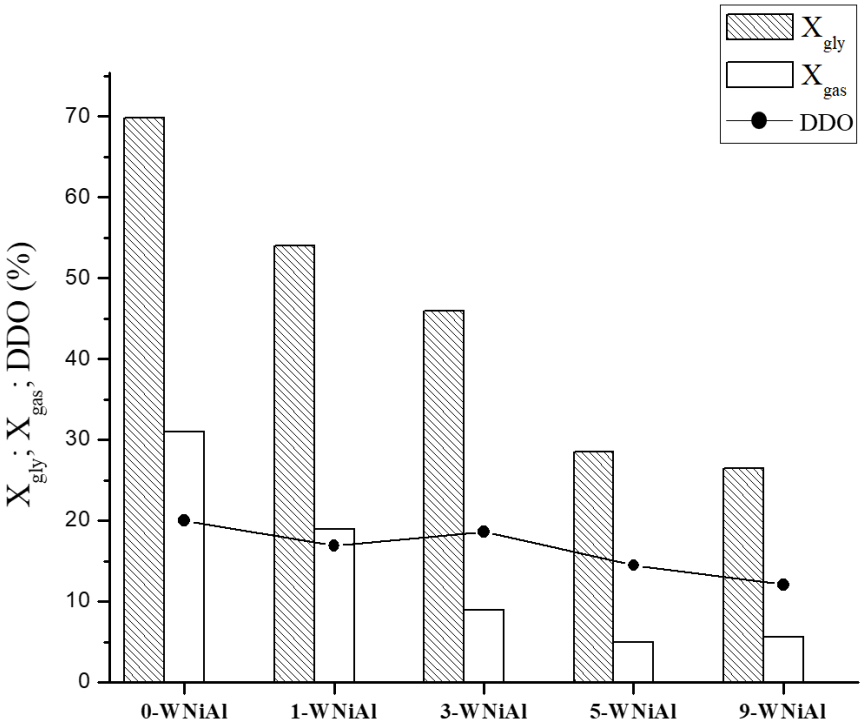

Figure 30. *Catalytic performance of x-WNiAl in glycerol HDO; Reaction condition: T = 235 °C, P = 45 bar.*

The catalyst which showed the best glycerol conversion was the not doped one, with a value that nearly reached the 70 %, while a moderate decrease of the values went together with the increase in tungsten content, reaching the minimum for the catalyst 9-WNiAl with 26.5% of glycerol conversion. The lower activity of W-doped catalyst in glycerol conversion can be attributed to different reasons. First, the bigger size of the formed Ni^0 crystallites, apart from 1-WNiAl, that also resulted in lower values of D_{Ni} (%), caused a lower availability of active metallic catalytic sites and an activity loss towards glycerol transformation. Second, the increasing high acidity of the systems made stronger the interaction between substrate and catalyst, but the low availability of the metallic sites made harder to break off the interaction and carry out the transformation. Last, the different interaction Ni-W, which as observed thanks to TPR analysis weakened the Ni-Al interactions, could also affect the activity in glycerol conversion.

The same trend observed for glycerol conversion, could be observed for carbon conversion to gas, where the X_{gas} for the catalyst 0-WNiAl resulted to be 31%, while the one for 9-WNiAl was 5%. This behaviour is easily explained by the higher density of total acidity of the doped catalysts: the glycerol conversion to gas through APR is activated by metallic sites, while the acid sites activate HDO, therefore, the glycerol converted gives more liquid products than gaseous ones, resulting in lower X_{gas} values with higher dopant contents.

The values of carbon from glycerol converted into liquid products were also calculated and are reported in ***Table 9***: the advantage of 0-WNiAl, when compared to 1-WNiAl, is not so notable.

Table 9*. Conversion of carbon from glycerol into liquid products for x-WNiAl catalysts.*

Catalyst	X_{liq}
0-WNiAl	48.2
1-WNiAl	43.8
3-WNiAl	41.8
5-WNiAl	28.4
9-WNiAl	25.1

In conclusion, W-doping was made with the purpose of promoting the conversion of glycerol into liquid products instead of gas, and so, enhancing the HDO process over the APR. Thus, even though the conversion of glycerol got worse, the lower results in carbon conversion to gas and the not significantly disadvantageous results in conversion to liquid products, suggested a positive effect of doping.

The purpose of the HDO reaction is to obtain high value-added liquid products with a lower O/C ratio with respect to glycerol, so they can be used as fuels and chemicals. For this reason, another interesting parameter to calculate for each catalyst was the degree of deoxygenation (DDO). A decrease of the value could be observed with the increase of tungsten content, making an exception for the catalyst 3-WNiAl, which showed a DDO value of 18.6%, really close to the 20% showed by 0-WNiAl.

Analysing the taken samples through gas chromatography (GC-FID), it was possible to identify the obtained compounds and to calculate the Carbon Selectivity (CS_i, %) for each obtained product. The results are shown in ***Table 10***, where the products belonging to Path I (from ***Figure 11***) require acid sites to occur, while the ones belonging to Path II require metallic sites.

Table 10. *Results of SC_i for each x-WNiAl catalyst.*

	SC_i (%)	***0-WNiAl***	***1-WNiAl***	***3-WNiAl***	***5-WNiAl***	***9-WNiAl***
PATH I	*Hydroxyacetone*	2.6	5.5	14.9	42.4	32.4
	Propylene glycol	33.8	41.8	48.2	0	29.3
	Acetone	0.3	0	0.6	0	0
	2-Propanol	31.1	0	0	0	0
	1-Propanol	0.5	0.3	0.5	0	0
	Propanoic acid	0	0	0	0	0.2
PATH II	*Ethylene glycol*	15.2	16.1	11.9	26.3	0.8
	Methanol	1.8	0.9	1.4	0	1.1
	Ethanol	0	10.8	17.8	1.8	13.3
	Acetic acid	0.7	0	0	0	0.2

Among all the identified products (acetaldehyde, acetone, methanol, 2-propanol, ethanol, 1-propanol, hydroxyacetone, acetic acid, propanoic acid, propylene glycol and ethylene glycol), the ones obtained in bigger quantities were hydroxyacetone (HA), propylene glycol (PG) and ethylene glycol (EG). In ***Figure 31*** the carbon selectivity results towards these three products are reported.

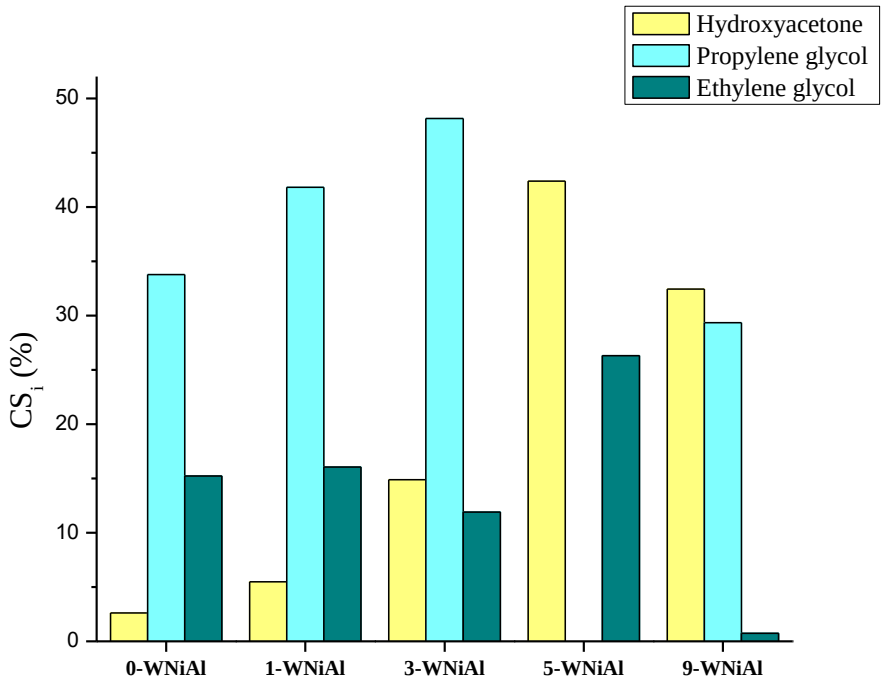

***Figure 31**. Carbon Selectivity to HA, PG and EG of x-WNiAl catalysts.*

Analysing the results of CS_{HA}, an increase of the values with the increase in tungsten content can be observed: this result perfectly accords with the fact that hydroxyacetone is the primary product of glycerol dehydration, therefore, the higher the surface acidity, the more HA is produced. Propylene glycol is a product of HA hydrogenation, and it needs metallic sites for being produced: this is why, looking at the CS_{PG} results, an increase of the values was shown by the catalysts with the bigger S_{Ni}^0, and lower values were shown by the catalysts with the highest tungsten loadings. For the production of ethylene glycol metallic sites are also required, since it is a secondary product of glycerol dehydrogenation, which gives glyceraldehyde, and subsequent decarbonylation on it. Coherently, the CS_{EG} value is about 15% for the not doped catalyst and nearly null for the 9-WNiAl. Overall, it was interesting to underline the higher values of CS_{PG} for 1-WNiAl and 3-NiAl when compared to 0-WNiAl, since propylene glycol is an interesting chemical to be produced. The two catalysts offered a good equilibrium between acid sites, necessary for the first step of dehydration to hydroxyacetone, and metallic sites, necessary for the second step of hydrogenation, enhancing the selectivity towards the desired product.

Apart from selectivity, efficiency towards the three main products was calculated considering the quantities of obtained products over the quantity of fed glycerol. The results are reported in ***Figure 32***.

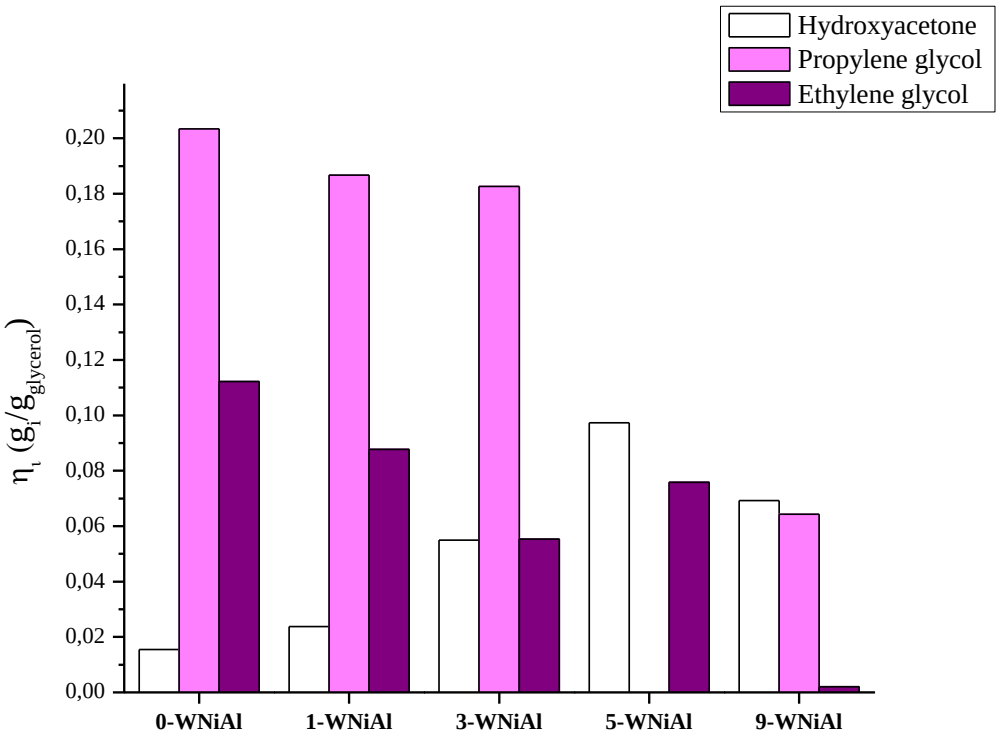

***Figure 32**. Efficiency values towards HA, PG and EG for each x-WNiAl catalyst.*

The trends showed by the different catalysts are quite similar to the ones for selectivity: they can be equally explained.

In conclusion, doping with tungsten helped the HDO reaction in terms of conversion into liquid products, but not in terms of glycerol conversion. For this reason, it was decided to choose the doped catalyst which showed the best performance (1W-NiAl) and to investigate on it, in order to achieve better results. Considering all together the parameters evaluated, the system with the 1 wt. % of tungsten was identified as the most interesting one: its X_{gly} was the highest among the doped catalyst and its X_{gas} was 39% lower than the X_{gas} of the not doped system. Furthermore, being the propylene glycol the most interesting product among the major three, also the relatively high values in terms of SC_{PG} and η_{PG} pushed in the direction of 1-WNiAl catalyst.

4.2.2 Effect of preparation method

To investigate if the preparation method could have had some effect on the performance of the system, and if it was possible to enhance it through this way, it was decided to synthesise the catalyst which was assumed to be the best, or better, the one with 1 wt. % of W, with a different technique, and to carry out the same studies as before. The catalyst was so synthesised via

impregnation, and the evaluations on conversion of glycerol, carbon conversion to gas and degree of deoxygenation were done and reported in ***Figure 33***.

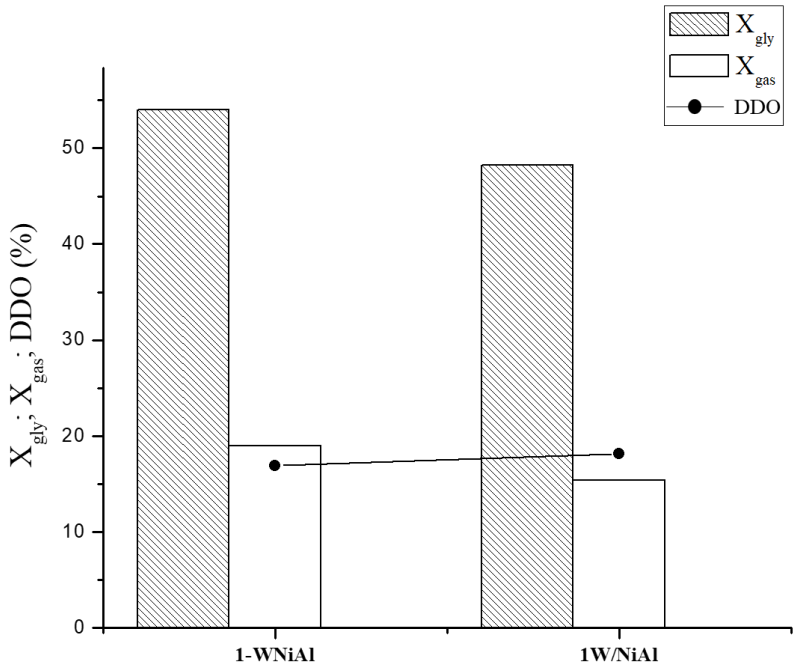

Figure 33. *Catalytic performance of 1-WNiAl and 1W/NiAl in glycerol HDO; Reaction condition: T = 235 °C, P = 45 bar.*

The catalyst synthesised via impregnation showed a slightly lower glycerol conversion value than the counterposed 1-WNiAl (48% vs. 54%), and again the reasons can be several. First, the bigger size of the Ni^0 particles formed and the subsequent lower value of D_{Ni}^0 for 1W/NiAl suggest a lower availability of metallic catalytic sites for glycerol conversion. Second, the way higher density of total acidity of the impregnated catalyst confirmed the effective lowering in availability of metallic sites.

The same reasons which explain the worsening in glycerol conversion, can also explain why 1W/NiAl presented a lower carbon conversion to gas and a higher degree of deoxygenation: the high acidity of the system enhanced even more the HDO reaction, making the performance more interesting than the one of the sol-gel catalyst.

Analysing the CS_i of the obtained compounds reported in ***Table 11***, it can be observed that the products obtained with the two systems are a little different in the amounts, but basically the same: this is a sign of the fact that the APHDO mechanism occurred during the two processes did not change.

***Table 11**. Results of SC_i for 1-WNiAl and 1W/NiAl.*

	SC_i (%)	***1-WNiAl***	***1W/NiAl***
PATH I	*Hydroxyacetone*	5.5	9.3
	Propylene glycol	41.8	50.3
	Acetone	0	0.4
	2-Propanol	0	0
	1-Propanol	0.3	0.4
	Propanoic acid	0	0
PATH II	*Ethylene glycol*	16.1	12.9
	Methanol	0.9	1.0
	Ethanol	10.8	13.6
	Acetic acid	0	0

In ***Figure 34***, the CS_i values given by the two systems for the three major products are shown. As discussed before, hydroxyacetone and propylene glycol production are favoured by acid sites, indeed, the impregnated catalyst showed a higher selectivity towards them. For ethylene glycol, which is favoured by metallic sites, coherently the system that showed a higher CS_{EG} value was the sol-gel synthesised.

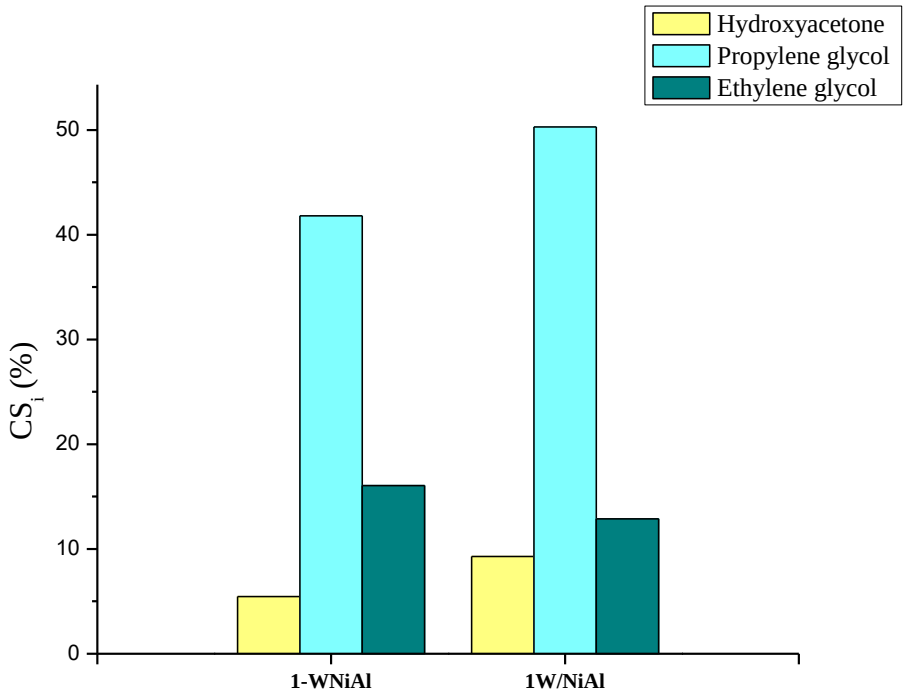

***Figure 34**. Carbon Selectivity to HA, PG and EG of x-WNiAl and 1W/NiAl.*

The efficiency was also evaluated and reported in ***Figure 35***. The trends, as before, are similar to the selectivity ones and can be equally explained.

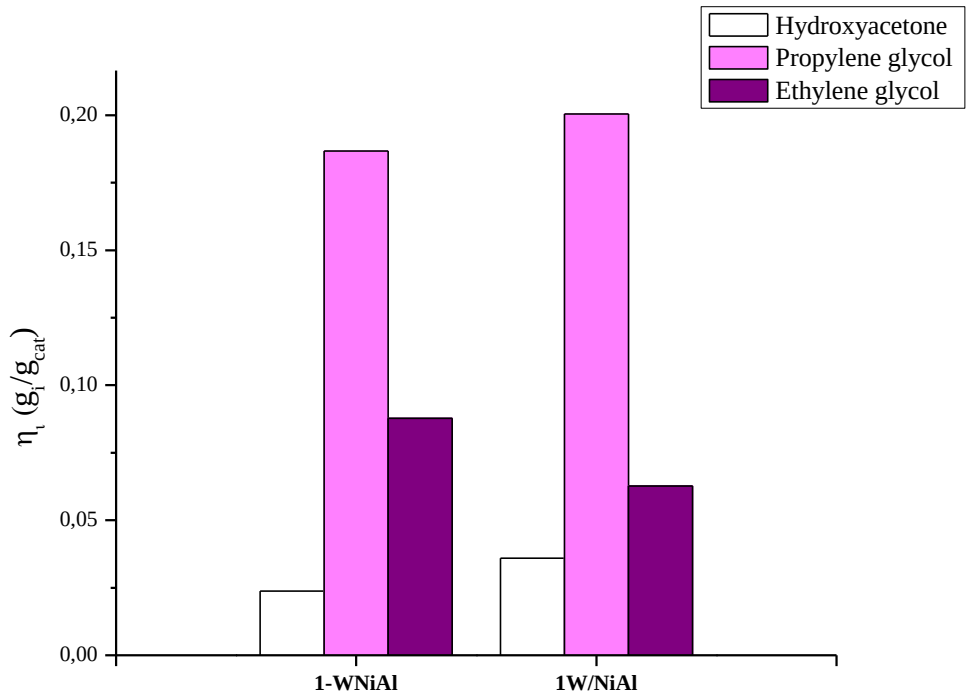

Figure 35*. Efficiency values towards HA, PG and EG for each x-WNiAl catalyst.*

In conclusion, 1W/NiAl gave a better performance than 1-WNiAl in terms of selectivity and efficiency, higher values of DDO and lower values of X_{gly} and X_{gas}. Besides, higher selectivity and efficiency towards propylene glycol can also be highlighted. Probably, the major quantity of tungsten present on the catalyst surface resulted in the major availability of the acid catalytic sites, therefore, in better activity in glycerol HDO reaction. The results obtained with 1W/NiAl are also good when compared to other works in literature, which studied the production of high value-added products (in particular, propylene glycol) through conversion of glycerol, without the use of external hydrogen, showing values in X_{gly} of 48.2% and in η_{PG} of 0.2 g/g_{cat}. The results of other works are reported in ***Table 12*** for the comparison in terms of glycerol conversion and efficiency in propylene glycol.

***Table 12**. Comparison with other works in literature which also studied the production of value-added profucts (propylene glycol) through glycerol conversion, without external hydrogen.*

Catalyst	***Conditions***	***Results***	***Reference***
28Ni/Al	227 °C, 34 bar, 10 wt. %, 3 h^{-1}, fixed bed	X_{gly} = 65.2 % η_{PG} = 0.169 g/g_{cat}	García et al.[82]
$CuNi/Al_2O_3$	250 °C, 40 bar, 10 wt. %, 2 h^{-1}, fixed bed	X_{gly} = 82 % η_{PG} = 0.198 g/g_{cat}	Freitas et al.[83]
CuNi/ZSM-5	250 °C, 40 bar, 10 wt. %, 2 h^{-1}, fixed bed	X_{gly} = 87 % η_{PG} = 0.223 g/g_{cat}	Freitas et al.[83]
5 Ru/Al_2O_3 + 5 Pt/Al_2O_3	220 °C, 14 bar, 10 wt. %, 0.083 g_{cat}/g_{gly}, batch	X_{gly} = 50.2 % η_{PG} = 0.196 g/g_{cat}	Roy et al.[37]
$65Ni/SiO_2$-Al_2O_3	240 °C, autogenous pressure, 10 wt. %, 0.25 g_{cat}/g_{gly}, batch	X_{gly} = 76 % η_{PG} = 0.065 g/g_{cat}	Seretis and Tsiakaras[84]
$28Ni/Al_3Fe_1$	227 °C, 34 bar, 10 wt.%, 3 h^{-1}, fixed bed	X_{gly} = 42.3 % η_{PG} = 0.178 g/g_{cat}	Raso et al.[85]

4.2.3 Effect of WHSV

Once assumed that the catalyst synthesised via impregnation with 1 wt. % of W worked the best, a further evaluation on the weight hourly space velocity parameter was done, in order to find a possible way to enhance even more the process. All the previous studies were conducted with a WHSV value of 1.2 g_{cat}/g_{gly}, utilising 0.5 g of catalyst and a feeding flow of glycerol of 0.1 mL/min: to evaluate the process with a WHSV of 2.4 g_{cat}/g_{gly}, the feeding flow was doubled to 0.2 mL/min while the catalyst mass was unchanged. All the other parameters, like temperature, pressure and time of sampling remained unchanged (T = 235 °C, P = 45 bar, 3 h). Firstly, the evaluations in terms of conversion of glycerol, carbon conversion to gas and deoxygenation degree were made and shown in ***Figure 36***.

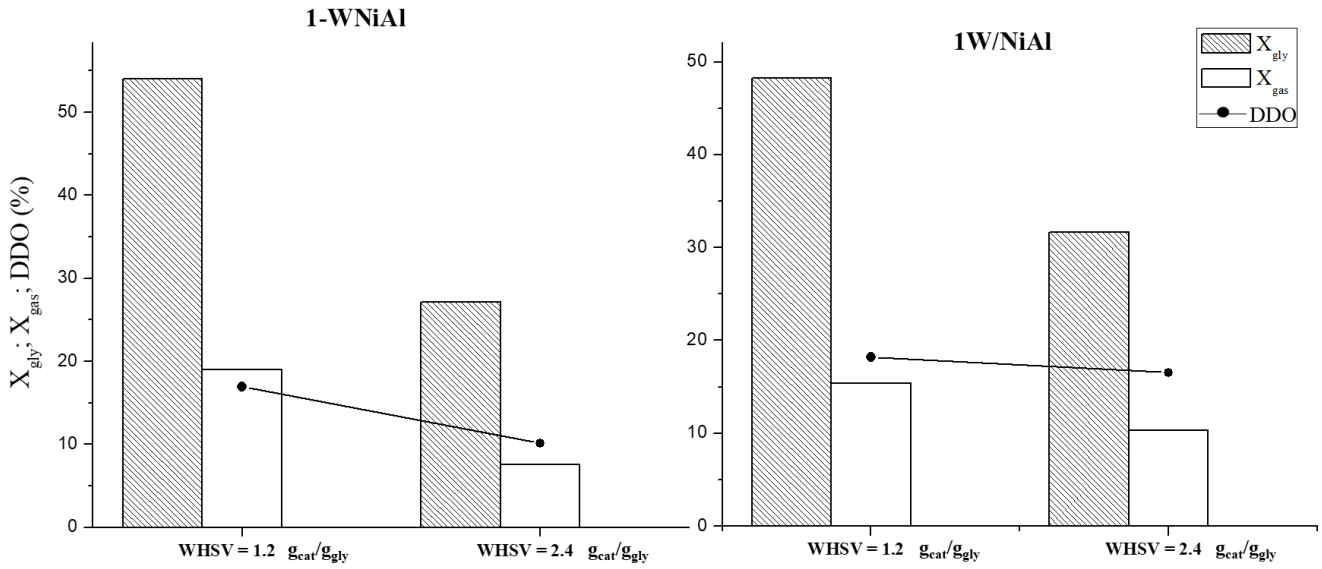

***Figure 36**. Catalytic performance of 1-WNiAl and 1W/NiAl in glycerol HDO with different WHSV; Reaction condition: T = 235 °C, P = 45 bar.*

Both in case of 1W-NiAl and 1W/NiAl, the increase of the WHSV parameter resulted in a lowering of all the calculated values. The X_{gly} decreased by 50% in case by 1-WNiAl (passing from 54% to 27%), and by 35% in case of 1W/NiAl (passing from 48% to 27%), motivated by the decrease in the contact time between glycerol and the active centres. The X_{gas} decreased by 41% in the first case (from 19% to 7.5%) and by 33% in the second (from 15% to 10%). Finally, the deoxygenation degree decreased by 41% for the former (from 17.0% to 10.1%) and by 10% for the latter (from 18.2% to 16.5%).

To evaluate a potential change in the reaction mechanism, and so in the obtained products and their distribution, the liquid outlet flow was analysed by gas chromatography and the calculated carbon selectivity values are reported in ***Table 11***:

***Table 11**. Results of SC_i for 1-WNiAl and 1W/NiAl tested with different WHSV.*

		1-WNiAl		***1W/NiAl***	
	SC_i (%)	***1.2 g_{cat}/g_{gly}***	***2.4 g_{cat}/g_{gly}***	***1.2 g_{cat}/g_{gly}***	***2.4 g_{cat}/g_{gly}***
	Hydroxyacetone	5.5	15.6	9.3	7.6
	Propylene glycol	41.8	13.2	50.3	53.4
PATH I	*Acetone*	0	0.3	0.4	0.3
	2-Propanol	0	21.9	0	0
	1-Propanol	0.3	0	0.4	0
	Propanoic acid	0	0	0	0
	Ethylene glycol	16.1	17.0	12.9	19.0
PATH II	*Methanol*	0.9	0.9	1.0	1.3
	Ethanol	10.8	0	13.6	18.5
	Acetic acid	0	0	0	0

The carbon selectivity to hydroxyacetone, propylene glycol and ethylene glycol, is shown in ***Figure 37***. When the WHSV parameter was doubled, in case of 1-WNiAl the CS_{HA} value showed a good increase, becoming almost three times higher (from 5.5 % to 15.5 %), while in case of 1W/NiAl the value slightly decreased from 9.3 % to 7.6 %. Looking at the CS_{EG} results, the selectivity did not change a lot among the four tests, maintaining a selectivity value around 12.9 and 19 %. The CS_{PG} showed a decrease by 60 % in case of the sol-gel synthesised catalyst, passing from a value of 41.8 % to 13.2 %, and a slight increase in the other case, passing from 50.3 % to 53.4 %.

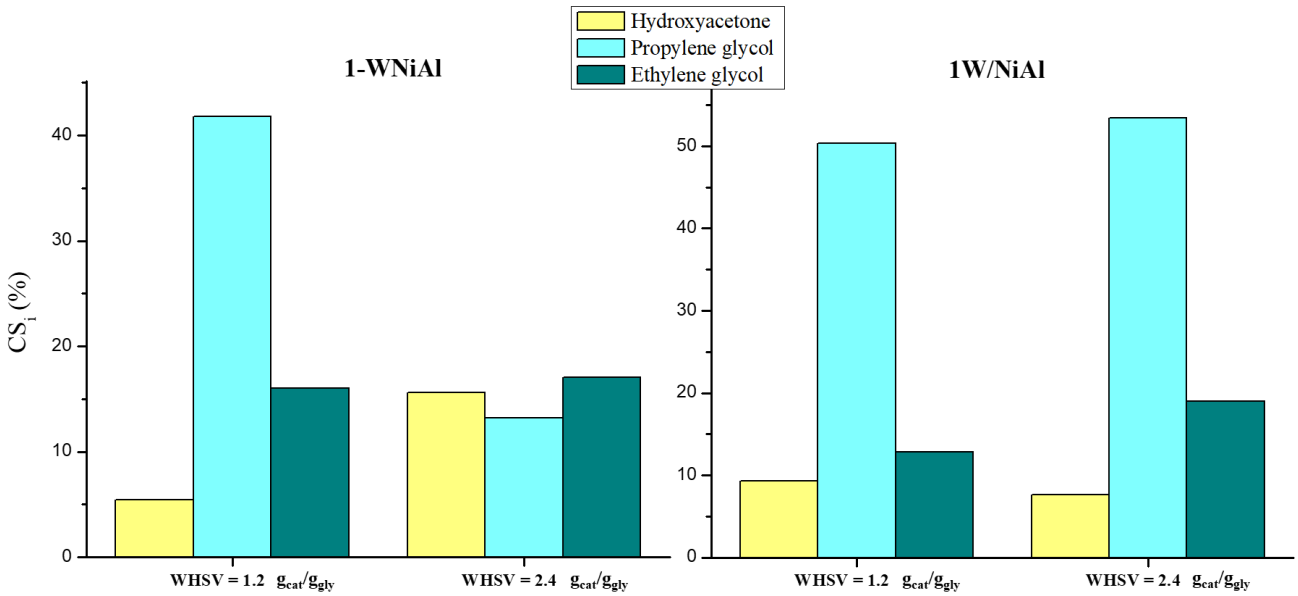

***Figure 37**. Carbon Selectivity to HA, PG and EG of x-WNiAl and 1W/NiAl, tested with different WHSV.*

Summarising, when the WHSV was changed to 2.4 g_{cat}/g_{gly}, for the sol-gel synthesised catalyst was likely the acid sites were promoted and the carbon selectivity towards hydroxyacetone increased, while the one towards propylene glycol hugely decreased; for the impregnated catalysts the opposite change is observed with a decrease in carbon selectivity to hydroxyacetone, and an increase in carbon selectivity to propylene glycol, suggesting a promotion of the metallic sites.

The efficiency of the catalysts in the four tests was also evaluated and reported in ***Figure 38***.

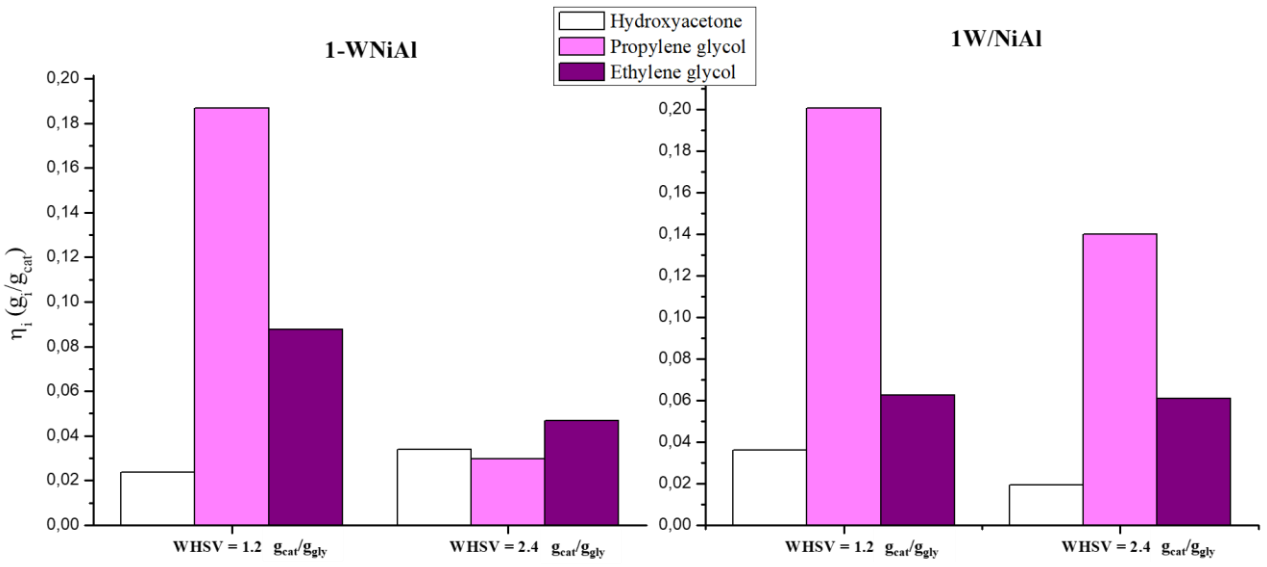

***Figure 38**. Efficiency in HA, PG and EG of x-WNiAl and 1W/NiAl, tested with different WHSV.*

The trends showed by efficiency, as in the previous cases, were very similar to the carbon selectivity ones, apart from the efficiency value for propylene glycol, which decreased for both the catalysts 1-WNiAl and 1W/NiAl when the WHSV is doubled.

In conclusion, the increase of the WHSV only resulted in a worsening of the catalysts performances, or better, the only parameters to be slightly improved were the carbon conversion to gas, the selectivity to hydroxyacetone in case of 1W/NiAl and to propylene glycol in case of 1W/NiAl. Looking at all the other parameters, from glycerol conversion to catalyst efficiency, for both the systems, the results suggested that it is better to keep a lower value of WHSV (i.e., higher contact time). Probably, when the feeding flow is lower, the substrate has more time to interact with the catalyst and to be subjected to the desired transformation.

5. GLOBAL VISION AND CONCLUSIONS

Doping the nickel aluminate catalytic system with tungsten had relevant effects on physicochemical properties and, subsequently, on its catalytic activity. The use of sol-gel synthesis method allowed the formation of WNiAl ternary oxides where tungsten was also hosted in the cubic spinel structure: the characterization results are a proof of it. Firstly, it could be deduced from the pore size distribution change: tungsten, caused the formation of bigger pores in the solids, which resulted in a shift of the pore size distribution to higher values of pore size when the amount of W added was bigger. Secondly, through the studies on reducibility of the solids, it could be highlighted that increasing the amount of W the reduction temperature got lower: probably, some W^{x+} ions replaced the Al^{3+} ions surrounding the Ni^{2+} in the spinel structure, causing a weakening of the Ni-Al interaction strength and a facilitation of the Ni^{2+} reduction. The weakening of the interaction between Ni and Al was also confirmed by the bigger dimensions of the Ni^{0} crystallites formed in the doped catalysts, which suggested a higher mobility of the reduced metal in the structure. Furthermore, after reduction and consequent metallic nickel crystallites formation, it was observed that the higher the W loadings, the smaller the metallic nickel dispersion values on catalysts surface obtained. In addition, the homogeneity of the structure (furnished by the sol-gel method) resulted in stable density of total acidity values among the differently loaded systems: the acidity increased together with the increase of W content, but its density remained about the same. Finally, W-doping also influenced the BET surface, making it to reach a maximum value when the 3 wt. % of W was added, and slightly lower values with bigger quantities.

From the catalytic point of view, doping unfavoured the conversion and the degree of deoxygenation of glycerol, but, as expected and desired, it was able to favour HDO over APR, showing every time for higher tungsten loadings lower conversion to gas values. Hydroxyacetone, propylene glycol and ethylene glycol resulted to be the major products and, calculating selectivity and efficiency towards them, the catalyst which showed the best performance was the one with the lowest amount of dopant (1 wt. %).

When the same catalyst was prepared with a different synthesis method, via impregnation, it showed different physicochemical properties and, subsequently, different catalytic performance. First of all, the two catalysts did not show a change in the pores size, but the sol-gel system seemed to be more resistant to the reduction process: indeed, after reduction, the pore size distribution remained quite the same for it, while for the impregnated one, a shift of

the parameter towards bigger dimensions could be observed. The impregnated catalyst resulted also generally easier to be reduced, showing a decrease of the reduction temperature of about 20 °C: somehow, the presence of WO_x species on the catalyst surface and not in the spinel structure, made the process easier. Moreover, the BET surface of the impregnated catalyst resulted to be about 30 % bigger than the sol-gel one, again because W was not intrinsically integrated in the spinel, but more on its surface. This "tungsten cover" also caused a lowering of the metallic nickel dispersion value, which resulted to be 7 times smaller with respect to the same sol-gel catalyst, and an increase of the acidity and its density: the impregnation method leaded to a bigger amount of W on the catalyst surface, resulting so in a bigger availability of the acid sites over the metallic ones.

The catalytic results confirmed the major and prompt availability of the acid sites with lower values of carbon conversion to gas, and with higher values of selectivity and efficiency towards hydroxyacetone.

In the end, the WHSV parameter was evaluated on both the sol-gel and the impregnated catalyst, and it was noted that, doubling the WHSV, a worsening of all the parameters evaluated was obtained, making an exception for the lowering of the carbon conversion to gas, which indicated a major conversion into liquid products. The doubled flow resulted in less available time for the reactant to interact with hydrogen, intermediate products and catalysts, thus, in lower conversion of glycerol and degree of deoxygenation.

To summarise, analysing the physicochemical data obtained, and relating them to the catalytic activity results, the following conclusions can be done:

- The W-doping of nickel aluminate catalytic systems had the effect of favouring the HDO process over the APR, leading to a higher production of liquid products than gaseous ones.
- W-doping enhanced HDO process, but generally made the catalysts less active towards conversion of glycerol. It is necessary to find a good compromise between the two parameters.
- Impregnation synthesis method leaded to a bigger availability of the acid catalytic sites, which consequently leaded to a major activity on HDO reaction and to a better selectivity and efficiency towards hydroxyacetone and propylene glycol.
- It is better to work under low values of WHSV to allow the substrate to interact with the catalytic sites and to be transformed.

The results obtained suggested a good effect of W-doping on HDO activation, but the results in terms of glycerol conversion needs to be enhanced. Other possible methods to add tungsten will be investigated, while substituting tungsten as dopant with other oxophilic metals, like molybdenum or niobium, is an alternative which is already being studied by the research group. Furthermore, the catalytic tests were only conducted over three hours: further studies will be conducted on long term reactions, in order to understand how the time can influence the process.

6. ACKNOWLEDGMENTS

(Ringraziamenti)

Quando nel mezzo di una pandemia anche essere accarezzato dal pensiero di andare al bar a prendere un caffè ti fa sentire un fuori legge, trovarti in viaggio per un nuovo paese ti fa sentire infinitamente fortunato: impaziente aspetti il decollo ed ogni centimetro del tuo corpo e della tua mente è pervaso dalla voglia di ringraziare tutti e tutto, anche il più piccolo granello di polvere per essersi posato esattamente lì dove l'ha fatto, che se magari si fosse posato un po' più là le cose sarebbero andate diversamente. Partendo dal granello di polvere e passando in rassegna tutti i contributi che hanno portato al suo culmine "l'effetto farfalla", dal più piccolo al più grande, arrivo a pensare a tutte le persone che hanno fatto e fanno parte di questa reazione a catena, velocissima e difficilissima da stoppare, e per ognuna di loro vorrei spendere qualche parola.

Grazie al professor Jose Luis Ayastuy per avermi accolto nel suo gruppo di ricerca ed essere stato sempre disponibile e presente, dal primo momento di smarrimento in un nuovo laboratorio, all'ultimo momento di stesura dell'elaborato.

Grazie a tutto il gruppo di ricerca TQSA per la disponibilità e l'aiuto offertomi durante la mia esperienza presso i suoi laboratori.

Grazie alla professoressa Patricia Benito Martin per avermi seguita durante la scrittura della tesi.

Grazie a Sara, per essere stata il mio braccio destro (o la mia mente) in tantissimi momenti, e per avermi trasmesso in questi anni la filosofia della lontra e la saggezza del bradipo.

Grazie a Lorenzo, per aver risposto sempre "certo ce beccamo" ad ogni mio singolo "Lo che fai, ti posso dare un po' fastidio?", diventando così una delle mie poche certezze.

Grazie a Myriam, per essere l'amica che è, nonché il mio amplificatore di personalità, che quando siamo insieme siamo tutto di più.

Grazie a Rocco, per non essersi mai stancato di ripetermi che non è importante essere sempre perfetti, ma è importante ascoltarsi ed essere sempre la migliore versione possibile di sé stessi, a seconda del momento.

Grazie a Nicolò, per rappresentare un modello di approccio "umanistico" e "strategico" alla vita al quale avvicinarmi, in quanto un po' lontana.

Grazie a Michele, per essere stato, forse inconsapevolmente, il mio faro in mezzo al mare di una notta scura, durante un anno in cui tutto è stato così, buio e nebbioso.

Grazie a Erika, per una infinitissima serie di ragioni, ma soprattutto per essere la persona che è, motivandomi ed ispirandomi continuamente.

Grazie a mamma e papà, per avermi sempre lasciata libera di scegliere e per avermi permesso di fare e di essere quello che voglio.

Grazie a tutta la mia famiglia ed a tutti i miei amici, per avermi accompagnata in questi anni ed aver contribuito a rendermi quello che sono adesso, regalandomi tutte quelle esperienze per cui la vita vale la pena di essere vissuta.

7. BIBLIOGRAPHY

(1) Biodiesel Production: Technologies, C., and Future Prospects Task Committee; Tyagi, R. D.; Y Surampalli, R.; C Zhang, T.; Yan, S.; Zhang, X. Biodiesel Production: Technologies, Challenges, and Future Prospects; *American Society of Civil Engineers* 2019.

(2) Jin, X.; Yin, B.; Xia, Q.; Fang, T.; Shen, J.; Kuang, L.; Yang, C. Catalytic Transfer Hydrogenation of Biomass-Derived Substrates to Value-Added Chemicals on Dual-Function Catalysts: Opportunities and Challenges; *ChemSusChem* 2019.

(3) Mäki-Arvela, P.; Murzin, D. Hydrodeoxygenation of Lignin-Derived Phenols: From Fundamental Studies towards Industrial Applications; *Catalysts* 2017.

(4) Werpy, T.; Petersen, G. Top Value-Added Chemicals from Biomass: Volume I -- Results of Screening for Potential Candidates from Sugars and Synthesis Gas; *National Renewable Energy Lab., Golden* 2004.

(5) Morales-Marín, A.; Ayastuy, J. L.; Iriarte-Velasco, U.; Gutiérrez-Ortiz, M. A. Nickel Aluminate Spinel-Derived Catalysts for the Aqueous Phase Reforming of Glycerol: Effect of Reduction Temperature; *Appl. Catal. B Environ.* 2019.

(6) Pagliaro, M.; Rossi, M.; Clark, J. H.; Kraus, G. A. Future of Glycerol; *Royal Society of Chemistry* 2010.

(7) Liu, X.; Yin, B.; Zhang, W.; Yu, X.; Du, Y.; Zhao, S.; Zhang, G.; Liu, M.; Yan, H.; Abbotsi-Dogbey, M.; Al-Absi, S. T.; Yeredil, S.; Yang, C.; Shen, J.; Yan, W.; Jin, X. Catalytic Transfer Hydrogenolysis of Glycerol over Heterogeneous Catalysts: A Short Review on Mechanistic Studies; *Chem. Rec.* 2021.

(8) Xu, W.; Niu, P.; Guo, H.; Jia, L.; Li, D. Hydrogenolysis of Glycerol to 1,3-Propanediol over a Al2O3-Supported Platinum Tungsten Catalyst with Two-Dimensional Open Structure; *React. Kinet. Mech. Catal.* 2021.

(9) Arandia, A.; Coronado, I.; Remiro, A.; Gayubo, A. G.; Reinikainen, M. Aqueous-Phase Reforming of Bio-Oil Aqueous Fraction over Nickel-Based Catalysts; *Int. J. Hydrog. Energy* 2019.

(10) Valliyappan, T.; Ferdous, D.; Bakhshi, N. N.; Dalai, A. K. Production of Hydrogen and Syngas via Steam Gasification of Glycerol in a Fixed-Bed Reactor; *Top. Catal.* 2008.

(11) Yang, G.; Yu, H.; Peng, F.; Wang, H.; Yang, J.; Xie, D. Thermodynamic Analysis of Hydrogen Generation via Oxidative Steam Reforming of Glycerol; *Renew. Energy* 2011.

(12) Lin, Y.-C. Catalytic Valorization of Glycerol to Hydrogen and Syngas; *Int. J. Hydrog. Energy* 2013.

(13) Adhikari, S.; Fernando, S.; Gwaltney, S. R.; Filip To, S. D.; Mark Bricka, R.; Steele, P. H.; Haryanto, A. A Thermodynamic Analysis of Hydrogen Production by Steam Reforming of Glycerol; *Int. J. Hydrog. Energy* 2007.

(14) Sánchez, E. A.; D'Angelo, M. A.; Comelli, R. A. Hydrogen Production from Glycerol on Ni/Al2O3 Catalyst; *Int. J. Hydrog. Energy* 2010.

(15) Iriondo, A.; Cambra, J. F.; Güemez, M. B.; Barrio, V. L.; Requies, J.; Sánchez-Sánchez, M. C.; Navarro, R. M. Effect of ZrO2 Addition on Ni/Al2O3 Catalyst to Produce H2 from Glycerol; *Int. J. Hydrog. Energy* 2012.

(16) Silva, J. M.; Soria, M. A.; Madeira, L. M. Challenges and Strategies for Optimization of Glycerol Steam Reforming Process; *Renew. Sustain. Energy Rev.* 2015.

(17) Adhikari, S.; Fernando, S. D.; Haryanto, A. Hydrogen Production from Glycerin by Steam Reforming over Nickel Catalysts; *Renew. Energy* 2008.

(18) Wang, W. Thermodynamic Analysis of Glycerol Partial Oxidation for Hydrogen Production; *Fuel Process. Technol.* 2010.

(19) Liu, S.; Lin, C. Autothermal Partial Oxidation of Glycerol to Syngas over Pt-, LaMnO3-, and Pt/LaMnO3-Coated Monoliths; *Ind. Eng. Chem. Res.* 2012.

(20) Song, Y.-Q.; He, D.-H.; Xu, B.-Q. Effects of Preparation Methods of ZrO2 Support on Catalytic Performances of Ni/ZrO2 Catalysts in Methane Partial Oxidation to Syngas; *Appl. Catal. Gen.* 2008.

(21) Guo, S.; Guo, L.; Cao, C.; Yin, J.; Lu, Y.; Zhang, X. Hydrogen Production from Glycerol by Supercritical Water Gasification in a Continuous Flow Tubular Reactor; *Int. J. Hydrog. Energy* 2012.

(22) Pairojpiriyakul, T.; Croiset, E.; Kiatkittipong, W.; Kiatkittipong, K.; Arpornwichanop, A.; Assabumrungrat, S. Hydrogen Production from Catalytic Supercritical Water Reforming of Glycerol with Cobalt-Based Catalysts; *Int. J. Hydrog. Energy* 2013.

(23) Xu, D.; Wang, S.; Hu, X.; Chen, C.; Zhang, Q.; Gong, Y. Catalytic Gasification of Glycine and Glycerol in Supercritical Water; *Int. J. Hydrog. Energy* 2009.

(24) Gutiérrez Ortiz, F. J.; Ollero, P.; Serrera, A.; Sanz, A. Thermodynamic Study of the Supercritical Water Reforming of Glycerol; *Int. J. Hydrog. Energy* 2011.

(25) Gutiérrez Ortiz, F. J.; Ollero, P.; Serrera, A. Thermodynamic Analysis of the Autothermal Reforming of Glycerol Using Supercritical Water; *Int. J. Hydrog. Energy* 2011.

(26) Schwengber, C.A.; Alves, H.J.; Schaffner, R.A.; da Silva, F.A.; Sequinel, R.; Rossato Bach, V.; Ferracin, R.J. Overview of glycerol reforming for hydrogen production; *Renew. Sustain. Energy Rev.* 2016.

(27) Aiouache, F.; McAleer, L.; Gan, Q.; Al-Muhtaseb, A. H.; Ahmad, M. N. Path Lumping Kinetic Model for Aqueous Phase Reforming of Sorbitol; *Appl. Catal. Gen.* 2013.

(28) Tuza, P. V.; Manfro, R. L.; Ribeiro, N. F. P.; Souza, M. M. V. M. Production of Renewable Hydrogen by Aqueous-Phase Reforming of Glycerol over Ni–Cu Catalysts Derived from Hydrotalcite Precursors; *Renew. Energy* 2013.

(29) Lin, Y.-C.; Huber, G. W. The Critical Role of Heterogeneous Catalysis in Lignocellulosic Biomass Conversion; *Energy Environ. Sci.* 2008.

(30) Rhodes, C.; Hutchings, G. J.; Ward, A. M. Water-Gas Shift Reaction: Finding the Mechanistic Boundary; *Catal. Today* 1995.

(31) Davda, R. R.; Shabaker, J. W.; Huber, G. W.; Cortright, R. D.; Dumesic, J. A. A Review of Catalytic Issues and Process Conditions for Renewable Hydrogen and Alkanes by Aqueous-Phase Reforming of Oxygenated Hydrocarbons over Supported Metal Catalysts; *Appl. Catal. B Environ.* 2005.

(32) Davda, R. R.; Shabaker, J. W.; Huber, G. W.; Cortright, R. D.; Dumesic, J. A. Aqueous-Phase Reforming of Ethylene Glycol on Silica-Supported Metal Catalysts; *Appl. Catal. B Environ.* 2003.

(33) Kirilin, A. V.; Tokarev, A. V.; Kustov, L. M.; Salmi, T.; Mikkola, J.-P.; Murzin, D. Yu. Aqueous Phase Reforming of Xylitol and Sorbitol: Comparison and Influence of Substrate Structure; *Appl. Catal. Gen.* 2012.

(34) Kim, T.-W.; Kim, H.-D.; Jeong, K.-E.; Chae, H.-J.; Jeong, S.-Y.; Lee, C.-H.; Kim, C.-U. Catalytic Production of Hydrogen through Aqueous-Phase Reforming over Platinum/Ordered Mesoporous Carbon Catalysts; *Green Chem.* 2011.

(35) Chheda, J. N.; Huber, G. W.; Dumesic, J. A. Liquid-Phase Catalytic Processing of Biomass-Derived Oxygenated Hydrocarbons to Fuels and Chemicals; *Angew. Chem. Int. Ed.* 2007.

(36) Akiyama, M.; Sato, S.; Takahashi, R.; Inui, K.; Yokota, M. Dehydration–Hydrogenation of Glycerol into 1,2-Propanediol at Ambient Hydrogen Pressure; *Appl. Catal. Gen.* 2009.

(37) Roy, D.; Subramaniam, B.; Chaudhari, R. V. Aqueous Phase Hydrogenolysis of Glycerol to 1,2-Propanediol without External Hydrogen Addition; *Catal. Today* 2010.

(38) Shahbudin, M. I.; Jacob, D. M.; Ameen, M.; Aqsha, A.; Azizan, M. T.; Yusoff, M. H. M.; Sher, F. Liquid Value-Added Chemicals Production from Aqueous Phase Reforming of Sorbitol and Glycerol over Sonosynthesized Ni-Based Catalyst; *J. Environ. Chem. Eng.* 2021.

(39) Yfanti, V.-L.; Lemonidou, A. A. Mechanistic Study of Liquid Phase Glycerol Hydrodeoxygenation with In-Situ Generated Hydrogen; *J. Catal.* 2018.

(40) Gandarias, I.; Arias, P. L.; Requies, J.; El Doukkali, M.; Güemez, M. B. Liquid-Phase Glycerol Hydrogenolysis to 1,2-Propanediol under Nitrogen Pressure Using 2-Propanol as Hydrogen Source; *J. Catal.* 2011.

(41) Barbelli, M. L.; Santori, G. F.; Nichio, N. N. Aqueous Phase Hydrogenolysis of Glycerol to Bio-Propylene Glycol over Pt–Sn Catalysts; *Bioresour. Technol.* 2012.

(42) Jin, W.; Pastor-Pérez, L.; Yu, J.; Odriozola, J. A.; Gu, S.; Reina, T. R. Cost-Effective Routes for Catalytic Biomass Upgrading; *Curr. Opin. Green Sustain. Chem.* 2020.

(43) Manfro, R.L.; da Costa, A.F. ; Ribeiro, N.F.P. ; Souza, M.M.V.M. Hydrogen production by aqueous-phase reforming of glycerol over nickel catalysts supported on CeO2; *Fuel Process. Technol.* 2010.

(44) García, L.; Ábrego, J.; Bimbela, F.; Sánchez, J. L. Hydrogen Production from Catalytic Biomass Pyrolysis. In *Production of Hydrogen from Renewable Resources*; Fang, Z., Smith, Jr., Richard L., Qi, X., Eds.; Biofuels and Biorefineries; Springer Netherlands: Dordrecht, 2015.

(45) Wen, G.; Xu, Y.; Ma, H.; Xu, Z.; Tian, Z. Production of hydrogen by aqueous-phase reforming of glycerol, *Int. J. Hydrog. Energy* 2008.

(46) Bindwal, A.B.; Vaidya, P.D. Toward hydrogen production from aqueous phase reforming of polyols on Pt/Al2O3 catalyst; *Int. J. Hydrog. Energy* 2015.

(47) Subramanian, N.D.; Callison, J.; Catlow, C.R.A., Wells P.P, Dimitratos, N. Optimised hydrogen production by aqueous phase reforming of glycerol on Pt/Al2O3, *Int. J. Hydrog. Energy* 2016.

(48) Tran, N. H.; Kannangara, G. S. K. Conversion of Glycerol to Hydrogen Rich Gas; *Chem. Soc. Rev.* 2013.

(49) Zhang, C.; Lai, Q.; Holles, J.H. Ir@Pt bimetallic overlayer catalysts for aqueous phase glycerol hydrodeoxygenation; *Appl. Catal. Gen.* 2016.

(50) Wei, Y.; Lei, H.; Liu, Y.; Wang, L.; Zhu, L.; Zhang, X.; Yadavalli, G.; Ahring, B.; Chen, S. Renewable Hydrogen Produced from Different Renewable Feedstock by Aqueous-Phase Reforming Process; *J. Sustain. Bioenergy Syst.* 2014.

(51) Manfro, R. L.; Pires, T. P. M. D.; Ribeiro, N. F. P.; Souza, M. M. V. M. Aqueous-Phase Reforming of Glycerol Using Ni–Cu Catalysts Prepared from Hydrotalcite-like Precursors. *Catal. Sci. Technol.* 2013.

(52) Iriondo, A.; Barrio, V. L.; Cambra, J. F.; Arias, P. L.; Güemez, M. B.; Navarro, R. M.; Sánchez-Sánchez, M. C.; Fierro, J. L. G. Hydrogen Production from Glycerol Over Nickel Catalysts Supported on Al2O3 Modified by Mg, Zr, Ce or La; *Top. Catal.* 2008.

(53) Remón, J.; Giménez, J.R.; Valiente, A.; García, L.; Arauzo, J. Production of gaseous and liquid chemicals by aqueous phase reforming of crude glycerol: Influence of operating conditions on the process; *Energy Convers. Manag.* 2016.

(54) Jiménez-González, C.; Boukha, Z.; de Rivas, B.; Delgado, J.J.; Cauqui, M.A.; González-Velasco, J.R.; Gutiérrez-Ortiz, J.I.; López-Fonseca, R. Structural characterisation of Ni/alumina reforming catalysts activated at high temperatures; *Appl. Catal. Gen.* 2013.

(55) Özdemir, H.; Öksüzömer, M.A.F.; Gürkaynak, M.A. Effect of the calcination temperature on Ni/MgAl2O4 catalyst structure and catalytic properties for partial oxidation of methane; *Fuel* 2013.

(56) Neto, A.S.B.; Oliveira, A.C.; Filho, J.M.; Amadeo, N.; Dieuzeide, M.L. de Sousa, F.F.; Oliveira, A.C. Characterizations of nanostructured nickel aluminates as catalysts for conversion of glycerol: Influence of the preparation methods, *Adv. Powder Technol.* 2016.

(57) Ribeiro, N.F.P.; Neto, R.C.R.; Moya, S.F.; Souza, M.M.V.M.; Schmal, M. Synthesis of NiAl2O4 with high surface area as precursor of Ni nanoparticles for hydrogen production; *Int. J. Hydrog. Energy* 2010.

(58) Yfanti, V.-L.; Ipsakis, D.; Lemonidou, A.A. Kinetic study of liquid phase glycerol hydrodeoxygenation under inert conditions over a Cu-based catalyst; *React. Chem. Eng.* 2018.

(59) Wawrzetz, A.; Peng, B.; Hrabar, A.; Jentys, A.; Lemonidou, A. A.; Lercher, J. A. Towards Understanding the Bifunctional Hydrodeoxygenation and Aqueous Phase Reforming of Glycerol; *J. Catal.* 2010.

(60) Liu, S.; Tamura, M.; Shen, Z.; Zhang, Y.; Nakagawa, Y.; Tomishige, K. Hydrogenolysis of Glycerol with In-Situ Produced H2 by Aqueous-Phase Reforming of Glycerol Using Pt-Modified Ir-ReOx/SiO2 Catalyst; *Catal. Today* 2018.

(61) Gandarias, I.; Requies, J.; Arias, P. L.; Armbruster, U.; Martin, A. Liquid-Phase Glycerol Hydrogenolysis by Formic Acid over Ni–Cu/Al2O3 Catalysts; *J. Catal.* 2012.

(62) Mauriello, F.; Ariga, H.; Musolino, M. G.; Pietropaolo, R.; Takakusagi, S.; Asakura, K. Exploring the Catalytic Properties of Supported Palladium Catalysts in the Transfer Hydrogenolysis of Glycerol; *Appl. Catal. B Environ.* 2015.

(63) Xia, S.; Zheng, L.; Wang, L.; Chen, P.; Hou, Z. Hydrogen-Free Synthesis of 1,2-Propanediol from Glycerol over Cu–Mg–Al Catalysts; *RSC Adv.* 2013.

(64) Cui, H.; Zayat, M.; Levy, D. Sol-Gel Synthesis of Nanoscaled Spinels Using Propylene Oxide as a Gelation Agent; *J. Sol-Gel Sci. Technol.* 2005.

(65) CRC Handbook of Chemistry and Physics: 1st Student Edition: Editor-in-Chief: R C Weast. CRC Press, Inc, Boca Raton, Florida and Wolfe Medical Publications, London. 1988; *Biochem. Educ.* 1989.

(66) Danks, A. E.; Hall, S. R.; Schnepp, Z. The Evolution of 'Sol–Gel' Chemistry as a Technique for Materials Synthesis; *Mater. Horiz.* 2016.

(67) Sing, K. S. W. Reporting Physisorption Data for Gas/Solid Systems with Special Reference to the Determination of Surface Area and Porosity (Recommendations 1984); *Pure Appl. Chem.* 1985.

(68) Lowell, S.; Shields, J. E.; Thomas, M. A.; Thommes, M. Characterization of Porous Solids and Powders: Surface Area, Pore Size and Density; *Springer Science & Business Media* 2012.

(69) Monson, P. A. Understanding Adsorption/Desorption Hysteresis for Fluids in Mesoporous Materials Using Simple Molecular Models and Classical Density Functional Theory; *Microporous Mesoporous Mater.* 2012.

(70) Thommes, M.; Cychosz, K. A. Physical Adsorption Characterization of Nanoporous Materials: Progress and Challenges; *Adsorption* 2014.

(71) Thommes, M.; Kaneko, K.; Neimark, A. V.; Olivier, J. P.; Rodriguez-Reinoso, F.; Rouquerol, J.; Sing, K. S. W. Physisorption of Gases, with Special Reference to the Evaluation of Surface Area and Pore Size Distribution (IUPAC Technical Report); *Pure Appl. Chem.* 2015.

(72) O'Neill, H. S. C.; Dollase, W. A.; Ii, C. R. R. Temperature Dependence of the Cation Distribution in Nickel Aluminate (NiAl204) Spinel: A Powder XRD Study; *Phys. Chem. Minerals* 1991.

(73) Li, G.; Hu, L.; Hill, J. M. Comparison of Reducibility and Stability of Alumina-Supported Ni Catalysts Prepared by Impregnation and Co-Precipitation; *Appl. Catal. Gen.* 2006.

(74) Braidy, N.; Bastien, S.; Blanchard, J.; Fauteux-Lefebvre, C.; Achouri, I. E.; Abatzoglou, N. Activation Mechanism and Microstructural Evolution of a YSZ/Ni-Alumina Catalyst for Dry Reforming of Methane; *Catal. Today* 2017.

(75) García-Sancho, C.; Guil-López, R.; Pascual, L.; Maireles-Torres, P.; Navarro, R. M.; Fierro, J. L. G. Optimization of Nickel Loading of Mixed Oxide Catalyst Ex-Hydrotalcite for H2 Production by Methane Decomposition; *Appl. Catal. Gen.* 2017.

(76) Boukha, Z.; Jiménez-González, C.; de Rivas, B.; González-Velasco, J. R.; Gutiérrez-Ortiz, J. I.; López-Fonseca, R. Synthesis, Characterisation and Performance Evaluation of Spinel-Derived Ni/Al2O3 Catalysts for Various Methane Reforming Reactions; *Appl. Catal. B Environ.* 2014.

(77) Garrido Pedrosa, A. M.; Souza, M. J. B.; Melo, D. M. A.; Araujo, A. S. Thermo-Programmed Reduction Study of Pt/WOx–ZrO2 Materials by Thermogravimetry; *J. Therm. Anal. Calorim.* 2007.

(78) Rogers, J. L.; Mangarella, M. C.; D'Amico, A. D.; Gallagher, J. R.; Dutzer, M. R.; Stavitski, E.; Miller, J. T.; Sievers, C. Differences in the Nature of Active Sites for Methane Dry Reforming and Methane Steam Reforming over Nickel Aluminate Catalysts; *ACS Catal.* 2016.

(79) Tirsoaga, A.; Visinescu, D.; Jurca, B.; Ianculescu, A.; Carp, O. Eco-Friendly Combustion-Based Synthesis of Metal Aluminates MAl2O4 (M = Ni, Co); *J. Nanoparticle Res.* 2011.

(80) Zhang, J.; Xu, H.; Jin, X.; Ge, Q.; Li, W. Characterizations and Activities of the Nano-Sized Ni/Al2O3 and Ni/La–Al2O3 Catalysts for NH3 Decomposition; *Appl. Catal. Gen.* 2005.

(81) Echeandia, S.; Arias, P.L.; Barrio, V.L.; Pawelec, B.; Fierro, J.L.G. Synergy effect in the HDO of phenol over Ni-W catalysts supported on active carbon: Effect of tungsten precursors; *Appl. Catal. B Environ.* 2010.

(82) García, L.; Valiente, A.; Oliva, M.; Ruiz, J.; Arauzo, J. Influence of operating variables on the aqueous-phase reforming of glycerol over a Ni/Al coprecipitated catalyst; *Int. J. Hydrog. Energy* 2018.

(83) Seretis, A.; Tsiakaras, P. Hydrogenolysis of glycerol to propylene glycol in continuous system without hydrogen addition over Cu-Ni catalysts; *Fuel Process. Technol.* 2016.

(84) Seretis, A.; Tsiakaras, P. Hydrogenolysis of Glycerol to Propylene Glycol by in Situ Produced Hydrogen from Aqueous Phase Reforming of Glycerol over SiO2–Al2O3 Supported Nickel Catalyst; *Fuel Process. Technol.* 2016.

(85) Raso, R.; García, L.; Ruiz, J.; Oliva, M.; Arauzo, J. Aqueous Phase Hydrogenolysis of Glycerol over Ni/Al-Fe Catalysts without External Hydrogen Addition; *Appl. Catal. B Environ.* 2021.